AD-A189 507 DEVELOPMENT OF ELECTROSTATIC-ACCELERATOR FREE-ELECRRON LASERS(U) CALIFORNIA UNIV SANTA BARBARA L R ELIAS 30 APR 87 N00014-80-C-0308 1/1

UNCLASSIFIED F/G 9/3 NL

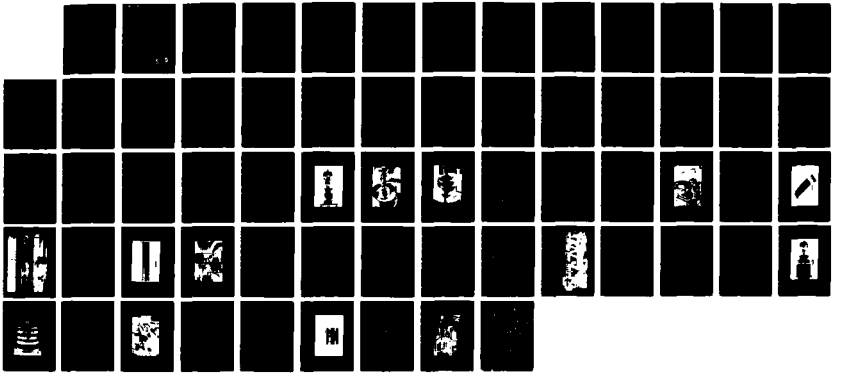

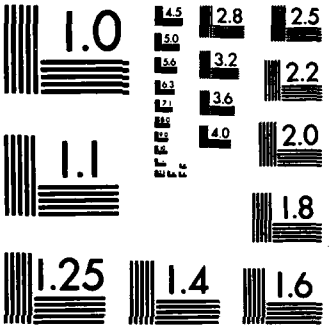

MICROCOPY RESOLUTION TEST CHART
NATIONAL BUREAU OF STANDARDS-1963-A

(4)

Development of Electrostatic-Accelerator Free-Electron Lasers

Principal Investigator: Luis R. Elias

University of California, Santa Barbara, CA 93106

Final Technical Report

ONR Contract N00014-80-C-0308

From January 15, 1980 through April 30, 1987

Table of Contents

		Page
A.	Introduction	2
B.	Phase I Accomplishments	6
	1. 2-Ampere Electron gun development	6
	2. 2-Ampere Electron collector development	7
	3. Beam recovery demonstration	8
	4. Electron beam transport system	9
	5. FIR resonator	10
	6. Undulator magnet	11
C.	Phase II Accomplishments	14
	1. Development of the UCSB electrostatic acc.	14
	2. First operation of the UCSB FEL	16
	3. Development of a hellically polarized magnet	17
	4. Resonator design for the first stage of the two-stage FEL	18
D.	Phase III Accomplishments	20
	1. Accelerator voltage upgrading	20
	2. Short wavelength FIR operation	20
	3. Single mode operation of the UCSB FEL	20
	4. 20-Ampere electron gun and electron collector	21
	5. 20-Ampere electron transport system	21
	6. First scientific utilization of an FEL	21
	7. Microundulator technology	22
	8. Electron beam analyzer	22
E.	Progress Reports	24
F.	Figures	30

A. INTRODUCTION

With support from the Office of Naval Research and the Air Force Office of Scientific Research, a free-electron laser has been developed at the University of California at Santa Barbara under ONR Contract N00014-80-C-0308. Its operation is based on the utilization of a 6 MV electrostatic accelerator which has been modified to generate relatively high current electron pulses of sufficient intensity to allow operation of free-electron lasers (FELs) as oscillators over a wide range of frequencies from the infrared (IR) to the far-infrared (FIR) region.

The evolution of the UCSB FEL has proceeded through a series of technical phases which began with the development of a unique, high current, high brightness electron gun in 1982, continued with the successful demonstration of very high electron beam recovery efficiency in 1983 and culminated with the operation of the FEL as an oscillator at wavelengths longer than 400 microns ~~in 1984~~, and with the demonstration of laser operation at wavelength longer than 120 micrometers after upgrading the accelerator voltage from 3 to 6 MV.

Since its initial conception, it has been the major goal of the ONR funded research program to develop a new breed of free-electron lasers based on the electron beams generated by electrostatic accelerators which would eventually be used as tools for scientific research in those regions of the spectrum where other coherent electromagnetic sources do not provide adequate power and/or continuous tunability.

Because of funding profile constraints, limited availability of laboratory space, and scarcity of technical manpower resources, it was decided, early in the program, that the UCSB research program should be carried out in three distinct, logically linked, consecutive technical phases. To carry out research in each phase of the program, a separate proposal was submitted to ONR.

Much of the design and construction of the FEL hardware was done at UCSB during Phase I. ~~However~~, initial testing of the hardware took place using a 3 MV accelerator made available to the FEL group at the National Electrostatic Corporation plant in Middleton, Wisconsin. The construction and assembly of the ~~UCSB~~ FEL, as well as the first operation of the FEL, took place in the ~~UCSB FEL~~ laboratory during Phase II. Finally, during phase III, the voltage of the accelerator was increased from 3 to 6 MV, in order to extend the operation of the FEL toward shorter wavelengths in the FIR region. The following is a summary of major research activities occurring during each technical phase of the program.

PHASE I (1/15/80-12/31/82)

- Development of a 2-Ampere electron gun and collector.
- Beam recovery demonstration.
- Beam quality measurements.
- Beam transport design and construction.
- Far-infrared resonator and undulator design and construction.

PHASE II (1/1/83-9/30/85)

- Acquisition and modification of a 3 MV accelerator.
- First demonstration of FEL operation in the 400-800 micron FIR region.
- Development of a helically polarized electromagnet for the first stage of a two-stage FEL.

PHASE III (10/1/85-3/31/87)

- Design and construction of the pump wave resonator of the two-stage FEL.
- Upgrading of electrostatic accelerator voltage from 3 to 6 MeV.
- FEL operation in the 120-800 micrometer region.
- Demonstration of single mode FEL operation.
- First utilization of an FEL in scientific research.

In the following sections, a summary of technical and scientific research carried out during each technical phase is presented as part of the final technical report. A more detailed description of research and development results carried out under this

contract can be found in 49 technical reports (see section F) submitted to ONR throughout the period of the contract.

B. PHASE I ACCOMPLISHMENTS

1. 2-Ampere electron gun development.

Nuclear research has been well served by particle beams generated by electrostatic accelerators. However, the current levels normally generated by these machines are too small to drive FELs, and consequently, new sources of electrons need to be developed.

The electron gun and the electron collector are perhaps the most critical components of an electrostatic-accelerator based electron beam system designed for beam recovery. Using his gun code, W. Herrmannsfeldt carried out the electrical design of the UCSB electron gun in 1980. Three major constraints were imposed on the electrical design: (1) the beam current should be close to 2 amperes, (2) the gun optics should be properly matched to NEC's electrostatic accelerator tube geometry and (3) the electron gun beam quality should be high. These requirements stem from the need to have a reasonably large FEL small signal gain and from the necessity of optimizing electron beam recovery. Figure 1 shows a photograph of one of two electron guns constructed for the project. Figure 2 shows its location inside the accelerator tank.

A summary of some of the important operating characteristics of the 2-ampere electron gun appear in Table I. Included in this table is data relating to the transverse phase space measurements conducted with the collaboration of Hughes Research Corporation, Electron Dynamics Division. Although, these measurements were made at a voltage of 10 kV, the table entry contains the normalized value of transverse emittance. The theoretical value of normalized transverse emittance was calculated using the well known formula derived by J.D. Lawson

$$\varepsilon_{\text{thermal}} = 2a[kT/mc^2]^{1/2},$$

for a cathode radius a, temperature T, and a constant current density distribution.

Table I. Operating characteristics of the 2-ampere UCSB electron gun.

Maximum beam current	2	Amperes
Maximum gun voltage	50	kV
Maximum grid voltage	10	kV
Cathode diameter	15.2	mm
Cathode temperature	1100	^{o}K
Output beam diameter	16	mm
Theoretical thermal emittance	9	π mm-mrad
Measured emittance	10	π mm-mrad

[a] Normalized emittance

2. 2-Ampere electron collector development.

The electron collector was designed to accept a 2 ampere electron beam with a maximum energy of 50 keV and a minimum energy of 40 keV. That is to say, it can accept a 10 kV energy spread. With regard to transverse phase space, the collector can accept a beam having a maximum transverse normalized emittance of 200π mm-mrad. The design geometry contains four collecting copper surfaces having 3.3 kV potential difference between consecutive surfaces. Its overall energy collecting efficiency of a 50

kV beam having a 10 kV voltage spread is nearly 95%. A photograph of the 2-Ampere collector installed inside the accelerator tank, is shown in Figure 3.

3. Beam recovery demonstration.

Beam recovery is important in electrostatic-accelerator FELs because the amount of HV charging current available in these machines is very small and the electrical capacitance of the HV terminal is also quite small. Typically only a few hundred microamperes of charging current can be generated with either a charging belt or pelletron chains and a maximum capacitance of 200 picofarads exists between the terminal shell and the high pressure accelerator tank. If more than the charging current is extracted as beam current from these devices, the terminal voltage will drop fast unless the beam is recovered.

Using a test electrostatic accelerator similar to that schematically shown in Figure 4, two critical technical tests were carried out at the National Electrostatic Corporation plant in Madison, Wisconsin.

The first test entailed a demonstration of beam recovery efficiency using the apparatus described in Figure 5. Once accelerated, the electron beam was transported through the 180 degree achromatic system shown in the figure. The electron beam is re-injected back into the decelerator tube shown in Figure 4 and then recovered by the electron collector.

The electron beam recovery rate R was calculated from the approximate formula $dV/dt = I_b (1-R)/C$, where dV/dt is the measured terminal voltage drop rate, I_b is the measured beam current, and C is the measured electrical capacitance of the terminal shell with respect to the grounded accelerator tank. Beam recovery results have been summarized in Table II.

As shown in Table II, the value of electron beam recovery efficiency is very nearly equal to 1. With improved beam optics development there is no technical

reason why these machines cannot be operated with continuous electron beams. In fact, with the geometry shown in the 2-MV accelerator of Figure 31, a 99.9% beam recovery rate is expected.

Table II. Beam recovery results.

Terminal voltage	2.5	MV
Beam current	1.2	Amperes
Charging current	200	Microamperes
Terminal capacitance	200	Picofarads
Maximum measured recovery rate	99.4	%
Terminal voltage droop rate		
with no recovery	6000	Volts/μ sec
with 99.4% recovery	36	Volts/μ sec

4. Electron beam transport system.

While the beam quality and beam recovery sections were completed, a new electron beam transport system was being developed to include the FEL undulator. H. Wiedemann helped design the hardware system shown in Figure 6. It consists of five 90^{o} achromatic bends and two sets of quadrupole magnets appropriately located to permit matching of the electron beam from the electrostatic accelerator to the FEL undulator. The bending magnets and quadrupoles)see Figure 7) were purchased from ANAC corporation of New Zealand. The initial electron beam transport tests were

carried out successfully at the NEC plant during February and March of 1983. However, the final FEL operation tests were conducted at UCSB in 1984.

5. FIR resonator.

The design of the UCSB resonator took into consideration three critically important features: a) large small signal gain, b) small cavity losses and c) flexibility to accommodate non-destructive electron beam diagnostic components.

A resonator geometry which fulfills all of the above design requirements was invented by the FEL group. It is shown in Figure 8. The basic geometry contains two cylindrical mirrors inserted between two stainless steel plates. In such a configuration, the cavity mode is guided in one direction by the plates, while in the perpendicular direction it is guided by the focussing properties of the cylindrical mirror. In this configuration the small signal gain is optimized because a) the mode area is small and b) the magnetic field produced by the undulator is large (i.e., the undulator gap is small).

Minimum resonator losses were obtained because the electric polarization of the fundamental mode is parallel to the guiding plates (i.e. minimum tangential magnetic field). The side plates do not contribute to losses because the amplitude of the fields drops exponentially away from the axis of the resonator.

Again because of the exponential drop of mode field strength away from the resonator axis in a direction parallel to the guiding plates, it was possible to install four pneumatically actuated fluorescent screens, which were used to diagnose electron beam position and size without introducing additional resonator losses in their out position. The output coupler consists of a small diameter copper mirror located inside the resonator with its normal oriented at 45^{o} with respect to the resonator axis. The design parameters of the resonator are listed in Table III.

Table III. Design parameters of the UCSB optical resonator.

Mirror geometry	Cylindrical	
Resonator length	712	cm
Mirror height	1.85	cm
Mirror radius of curvature	500	cm
Mirror width	10	cm
Wavelength	380	μm
Average mode area	2.4	sq. cm
Mode waist radius (86% energy)	1.17	cm
Small signal gain	1	
Theoretical losses	0.6	%
Outcoupler losses	20	%

6. Undulator magnet.

The undulator consists of 1280 Samarium-Cobalt rectangular magnets arranged in a Halbach configuration. Mechanical support is provided by five sets of aluminum honeycomb panels, each containing 32 periods. Magnets for each period are attached to aluminum carrier plates, in groups of four, by Beryllium-Copper springs as shown in Figure 9. An adjustable gap is achieved by supporting the honeycomb panels with lead screws driven by a ladder chain running around the whole undulator, as can be seen in Figure 10. Lateral position is defined by linear ball bearings. The individual magnets were composed of three glued pieces which were sheathed in 8 mill stainless steel

sheets for protection against breakage. A diagram describing the major components of the undulator is shown in Figure 11, Figure 12 shows a topview photograph of the assembled undulator with the top panel off. The undulator can be seen in Figure 13 near (and parallel to) the left wall. The accelerator tank is seen in the background and to the right, the two-stage FEL to be described later on.

The undulator's 1280 magnets were selected from a group of 1500 magnets. Flux measurements were first made on each individual magnet at a distance of 2 cm from each side of a magnet. The selection procedure then involved arranging magnets in groups of four. One vertically oriented pair and one horizontally oriented pair were then assembled onto two carrier plates to make one period. The reasoning behind this procedure was that if magnets of each orientation, oppositely located in the array, were matched, then any asymmetries resulting from nonuniform magnetization would tend to cancel. A final selection of plates was done based on the magnetic fields generated by each period plate .

The magnetic fields were measured using a Hall probe. Figure 14 shows the behavior of the transverse field on axis of a 32 period section.

Table IV summarizes some important parameters of the UCSB undulator.

Table IV. UCSB undulator parameters

Period length	3.6	cm
Number of periods	160	
Undulator length	576	cm
Undulator gap	3-9	cm
Peak magnetic field on axis	5-760	Oersted
Magnet dimensions		
length	10	cm
width (square)	0.85	cm
Material	H90B Samarium-Cobalt	
Manufacturer	*Hitachi*	
Residual field	0.87	Tesla
Coercive force	16000	Oersted

A beam envelope equation was used to study the propagation of the electron beam through the magnetic undulator. A typical beam envelope computer simulation is illustrated in Figure 15. The periodicity in the beam envelope is associated with the betatron motion of the electrons resulting from the transverse focussing of the undulator.

C. PHASE II ACCOMPLISHMENTS

Having completed the construction of most of the FEL hardware during phase I, and having concluded with the beam recovery and beam quality tests at the NEC plant in 1983, the FEL hardware was transported back to Santa Barbara, where it was reassembled inside the newly completed UCSB FEL laboratory facility. That same year the newly constructed UCSB electrostatic accelerator was installed in the laboratory.

1. Development of the UCSB electrostatic accelerator.

The major components of the UCSB electrostatic accelerator are shown in Figure 4. Included among these are:

- Electron gun
- Electron collector
- Accelerator tube
- Decelerator tube
- HV charging system
- Shielded terminal electronics
- Electrical power system for terminal electronics

The electron gun and electron collector have been described previously. The accelerator tube is of the standard NEC high gradient version. Beam matching between the electron gun and the accelerator tube was accomplished with the use of Herrmansfeldt's gun design program. Beam transport through the accelerator tube was studied using a beam envelope equation containing radial space charge forces and electrostatic forces generated by the accelerator tubes. Figure 16 describes the final matched beam optics inside the accelerator tube. It is important to realize that the

electron beam is confined within the accelerator tube due to prescribed electrostatic forces alone. No magnetic confining forces, such as a longitudinal magnetic field, were required. Within the decelerator tube the beam envelope equation was used to determine the matching properties of the decelerator tube to that of the electron collector and to the external transport system. The transport and matching properties of the electron beam with the FEL undulator has also been discussed in previous sections of this report.

The original accelerator contained sufficient sections to operate it with a maximum voltage of 3 MV. However, from the beginning, the accelerator tank was designed to accept a 6 MV accelerator. Electrical power to the HV terminal is derived from electrical generators located inside the terminal shell. The generators are mechanically driven by an insulating plastic shaft extending along the axis of the accelerator tank rotating at a 800 rpm rate. Electrical insulation inside the accelerator tank is provided by SF_6 gas held at a pressure of 70-80 psi.

The accelerator HV power supply consists of two pelletron chains capable of delivering up to 200 μA of charging current. Voltage regulation of the accelerator was obtained using a generating voltmeter to sense the terminal voltage and a corona triode regulator located inside the HV terminal.

Table V lists the major operating characteristics of the accelerator.

Table V. Operating characteristics of the UCSB electron beam system as of 1987.

Maximum terminal voltage	6	MV
Maximum beam current	2.4	Amperes
Maximum electron pulse length	50	μseconds
Maximum pulse repetition rate	1	Hz
Maximum beam recovery		
laser off	97	%
laser on	95	%
Pulse/pulse voltage stability	0.05	%

2. First operation of the UCSB FEL.

The first operation of the UCSB FEL as a far-infrared oscillator occurred on August 22, 1984. Figures 17 and 18 show oscilloscope traces of power vs. time for a short and for a long electron pulse respectively. The upper traces show the electron beam current time structure for each case. The laser power fluctuations seen in Figure 18 are associated with longitudinal mode jumping due to the finite voltage droop of the accelerator voltage, which in turn is associated with the finite electrical HV terminal capacitance. Results of the first operation have been included in Table VI.

Table VI. Results of the first operation of the UCSB FEL

Laser frequency	750	GHz
Laser wavelength	400	μm
Wavelength tuning range	400-800	μm
Maximum estimated power	10	kW
Laser small signal gain	30	%
Resonator losses	11	%
Power e-folding time	300	ns
Time to reach saturation	4	μs
Maximum pulse length	35	μs

Laser gain and resonator losses were calculated from cavity power risetime and decay time measurements. Measured resonator power losses (mainly coupling losses) agree well with calculated values. However, laser gain measurements were down by a factor of three when compared with the calculated value. With proper tuning the small signal gain increased to 100% per pass in 1986

3. Development of a helically polarized electromagnet.

The helically polarized electromagnet shown in Figure 19 was built to function as the undulator for the first stage of a two-stage FEL. Guiding aluminum pieces were attached to a stainless steel tube to form the mandrel for a bifilar helical winding. Altogether, 88 loops of copper wire were used to cover the helical mandrel. Tapering of the end fields was achieved by reducing the number of wire layers by one every quarter turn. The design parameters of the undulator are listed in Table VII.

Table VII. Parameters of the UCSB helical undulator.

Magnet polarization	Helical	
Magnet period	20	cm
Magnet aperture	8.8	cm
Number of periods	14	
Maximum peak field (on axis)	200	Oersted
Undulator parameter	0.373	
Maximum winding current	40	Amperes
Cooling	Forced air	
Number of wires/layer	11	
number of layers	8	

The magnetic field homogeneity of the helical undulator is exceptionally good. A plot of transverse field on axis is shown in Figure 20, while the dependence of field amplitude with radial distance is displayed in Figure 21. The dashed and continuous lines correspond to the fundamental harmonic and full field respectively, whereas the points correspond to experimental measurements. There is very good agreement between theory and experiment.

4. Resonator design for the first stage of the two-stage FEL.

In order to minimize pump wave resonator losses for the first stage of the two-stage FEL, a free space mode configuration was chosen for the pump wave. A diagram

of the resonator optics for both stages can be found in Figure 22. The resonator parameters of the pump wave are listed in Table VIII.

Table VIII. Resonator parameters for the pump wave of the two-stage FEL at a voltage of 6 MV.

Mode wavelength	703	mm
Mirror radius of curvature	3.8	m
Resonator length	5.4	m
Mode waist radius	2	cm
Rayleigh length	1.75	m
Fresnel number	0.73	
Saturation power density	4.6×10^7	watts/cm^2
Resonator losses	3	%

The design values shown in Table VII were chosen in order to maximize the small signal gain of both the pump wave and the two-stage wave. Most of the resonator losses are due to the finite absorption of copper in the FIR region. The theoretical reflectivity of copper in the FIR is approximately 99.7, assuming the dc value of conductivity of copper. The saturation optical power density of the pump wave corresponds to wave magnetic field of 400 oersted.

D. PHASE III ACCOMPLISHMENTS

1. Accelerator voltage upgrading.

From the beginning of the UCSB FEL program it was understood that the electrostatic accelerator would eventually reach a maximum energy of 6 MeV. Too that effect additional accelerator and decelerator sections were added late in 1985 to reach a maximum terminal voltage of 6 MV.

At higher voltage the accelerator can produce internal electrical arcs which can produce serious damage to those electrical components located inside the high-voltage terminal. It was, thus, necessary to harden all electrical equipment which could be sensitive to arc damage. It took nearly 2 months of work to protect them from arc damage at 5.5 MV.

2. Short wavelength FIR operation.

As a result of increased electrostatic accelerator voltage, the UCSB FEL has been tuned over an unprecedentedly wide region of the spectrum, from 120 to 800 microns. This range constitutes a factor of nearly seven in frequency. By comparison, the visible spectrum covers only a factor of two in frequency.

3. Single mode operation of the UCSB FEL

Because of 0.05 % pulse-to-pulse voltage fluctuations in the accelerator terminal, the narrow frequency spectrum of single FEL pulse was obscured. The voltage fluctuations gave rise to 0.1 % pulse-to-pulse FEL frequency fluctuations. However, using a fast Shottky-diode receiver, it was possible to measure the frequency bandwidth of a single laser pulse. From time domain measurements the fractional bandwidth of a single FEL pulse is approximately 5×10^{-8} ! Thus, unlike other

operating FELs, and because of its long electron pulses, the UCSB FEL operates with an extremely narrow bandwidth.

4. 20-Ampere electron gun and electron collector.

In order to drive the two-stage FEL above threshold it is necessary to increase the current carrying capabilities of the accelerator from 2 to 20 amperes. As part of this work two 200 kV electron guns and one 200 kV electron collector has been developed. The electron gun and collector are shown in Figure 23 and 24.

5. 20-Ampere electron transport system.

The Phase II electron beam transport system was originally designed for a maximum beam current of 2 amperes. However, the two-stage requires 20 amperes of beam current for their operation. Thus, the electron beam transport system was modified to accept the 20-Ampere beam current on the two-stage beamline schematically shown in Figure 25. As shown in the figure the new beamline has also been designed for electron beam recovery. Figure 26 shows the hardware for the first stage of the two-stage FEL.

With the above described beamline modifications, the 6 MV accelerator can operate in conjunction with either of the two FELs attached to it.

6. First scientific utilization of an FEL.

During this phase III, the stable operation of the UCSB FEL has led to the first application of an FEL to scientific research. The group of Dr. Vincent Jaccarino, at UCSB, has measured the transmission spectra of a FeF_2. In the past, before the UCSB began operation, it was possible to study the FIR spectra of crystals only at those fixed

frequencies where molecular lasers happen to operate. The results are shown in Figure 27.

7. Microundulator technology.

The idea of microundulators was first introduced by the UCSB FEL group, during technical Phase III of the program.

Conventional undulators, such as the Halbach structure used in the UCSB FEL, consists of individual magnets with dipole moment successively rotated by 90 degrees. Recognition of the difficulty of handling individual magnets of the dimensions required by a short period undulator, motivated the development of alternate configurations known as microundulators. These structures consist of grooves milled in large blocks of magnetized material. Periods as short as 1 mm appear possible. Two feasible microundulator configurations are shown in Figures 28 and 29. Figure 30 shows a test microundulator section.

With microundulators it will be possible to obtain short wavelength radiation using relatively low energy accelerators. The machine shown schematically in Figure 32 is an example of a compact FEL which could be used in the FIR region using a 2 MV electrostatic accelerator.

8. Electron beam analyzer.

The quality (i.e. small transverse emittance) of the beams generated by the UCSB electron guns is difficult to measure because of strong radial space charge forces. Even using beam analyzer technology developed by Hughes Research Corporation, it was difficult to extract the transverse temperature of the electron beam generated by the 2-Ampere electron gun. With partial support of an ONR DURIP

grant a "state of the art" electron beam analyzer is being constructed. A photograph of the hardware is shown in Figure 32.

E. PROGRESS REPORTS

The following publications have been sent to the ONR mail list according to instructions in ONR contract NOOO14-80-C-0208 January 1980-December 1986.

QIFEL004/80: ELECTROSTATIC ACCELERATOR FREE ELECTRON LASERS, L.R. ELIAS, PUBLISHED IN THE FREE ELECTRON LASER, ed. S. MARTELLUCCI, A. CHESTER, p. 617, PLENUM PRESS 1983.

QIFEL005/80: THE UCSB FEL EXPERIMENTAL PROGRAM, L. ELIAS PUBLISHED IN THE FREE ELECTRON LASER, ed. S. MARTELLUCCI, A. CHESTER, p. 321, PLENUM PRESS 1983.

QIFEL009/81: COHERENT LIENARD-WIECHERT FIELDS PRODUCED BY FELS, (ELIAS, GALLARDO), PHYS. REV. A24, 3276, DECEMBER 1981.

QIFEL011/81: DESIGN OF THE UCSB FEL ELECTRON BEAM SYSTEM (ELIAS, RAMIAN), PHYS. OF QUANTUM ELECT., VOL. 9, 577, ed. GERALD T. MOORE, 1982.

QIFEL012/81: THREE DIMENSIONAL ELECTROMAGNETIC FIELDS IN FELS, (ELIAS, GALLARDO), PHYS. OF QUANTUM ELECT., VOL. 9, 603, ed. GERALD T. MOORE, 1982.

QIFEL017/83: CYLINDRICAL GAUSSIAN-HERMITE MODES IN RECTANGULAR WAVEGUIDES RESONATORS (Elias, Gallardo) APPLIED PHYS. B 31, 299, 1981.

QIFEL018/83: RESULTS OF THE UCSB FEL ELECTRON BEAM RECIRCULATION EXPERIMENT (Elias, Ramian), PROCEEDINGS OF THE INTERNATIONAL CONFERENCE OF LASERS '82, 154, 1983.

QIFEL019/83: TRANSPORT PROPERTIES OF RELATIVISTIC ELECTRON BEAMS THROUGH LINEARLY POLARIZED MAGNETIC WIGGLERS (Hu, Elias) PROCEEDINGS OF THE INTERNATIONAL CONFERENCE OF LASERS '82, 171, 1983.

QIFEL021/83: RADIATION MEASUREMENTS FOR UCSB-FEL (BOSCOLO, ELIAS, RAMIAN) PROCEEDINGS OF THE INTERNATIONAL CONFERENCE OF LASERS '82, 159, 1983.

QIFEL022/83: EFFECTS OF RECTANGULAR BOUNDARIES ON THE RADIATION FIELD OF A LINEARLY POLARIZED WIGGLER FREE ELECTRON LASER, (AMIR, ELIAS) LASERS IN FLUID MECHANICS AND PLASMA-DYNAMICS AIAA, 159, JULY 1983.

QIFEL023/84: PROPERTIES OF THE UCSB FEL WIGGLER (ELIAS, RAMIAN AND R-C HU) INT'L SOC. FOR OPTICAL ENGINEERING, VOL. 453, 160, 1984.

QIFEL024/84: CYLINDRICAL GAUSSIAN EIGENMODES OF A RECTANGULAR WAVEGUIDE RESONATOR THREE-DIMENSIONAL NUMERICAL CALCULATION OF GAIN PER MODE (AMIR, ELIAS, GALLARDO) INT'L SOC. FOR OPTICAL ENGINEERING, VOL. 453, 235, 1984.

QIFEL025/84: STATUS REPORT OF THE UCSB FEL (ELIAS, RAMIAN) INT'L SOC. FOR OPTICAL ENGINEERING, VOL. 137, 453, 1984.

QIFEL026/83: ENERGY EXTRACTION FROM THE ELECTRON BEAM IN A FEL RESONATOR GAUSSIAN MODE (ELIAS, GALLARDO, GOLDSTEIN) PROCEEDINGS OF THE INTERNATIONAL CONFERENCE OF LASER '82, 1983.

QIFEL027/84: SMALL-SIGNAL GAIN OF A FEL IN A RESONATOR GAUSSIAN MODE (BOSCOLO, GALLARDO) APPL. PHYS. B 35, 163, 1984.

QIFEL028/84: ANALYSIS OF THE SPHERICAL RAMAN-NATH EQUATION (BOSCO, DATTOLI, GALLARDO) J. PHYS. A17, 2739 1984.

QIFEL030/84: FREE ELECTRON LASERS (Luis Elias) The Future of lightwave Technology, NSF Workshop Concerning Quantum Electronics, eds. M. Bass and E. Garmire, 38, Feb. 1984. (NOT PUBLISHED)

QIFEL032/84: A SUBMILLIMETER FEL (ELIAS) 9th INTERNATIONAL CONFERENCE ON INFRARED AND MILLIMETER WAVES, 1985.

QIFEL034/84: THE SPHERICAL RAMAN-NATH EQUATIONS WITH TIME-DEPENDENT COEFFICIENTS
(Dattoli, Gallardo. TORRE)
Lettere al Nuovo Cimento, 42, 163, 1985.

QIFEL035/84: QUANTUM STATISTICAL PROPERTIES OF AN FEL AMPLIFIER
(Dattoli, Gallardo, Renieri, Richetta)
IEEE Journal of Quantum Electronics Special Issue on Fels, 1985.

QIFEL036/84: QUANTUM COHERENCE PROPERTIES OF THE FEL
(Dattoli, Gallardo, Richetta, Torre)
Nuclear Instruments and Methods in Physics Research, 1985.

QIFEL037/84: QUANTUM MULTIMODE ANALYSIS OF THE FEL
(Dattoli, Gallardo, Torre)
Phys. Rev. A, 31, 6, 1355-3760 1985.

QIFEL038/84: PHOTON STATISTICAL PROPERTIES OF AN OPTICAL WIGGLER FEL
(Dattoli, Gallardo, Torre)
J. of the Opt. Soc. B, VOL.3 65-67 JAN. 1985

QIFEL040/85: SCIENTIFIC RESEARCH WITH THE UCSB FEL
(Elias, Jaccarino, Yen)
Nuclear Instruments and Methods in Physics Research, A239, 439 1985.

QIFEL041/85: FAR-INFRARED, LOW-LOSS, CYLINDRICAL-GAUSSIAN EIGENMODES OF A BENT RECTANGULAR WAVEGUIDE FEL RESONATOR
(Elias, Gallardo, Kimel)
Journal of Applied Physics, 57 (11) June 1985.

QIFEL043/85: MICRO-UNDULATOR FEL TECHNOLOGY
(Elias, Ramian)
Proceedings of the International Conference of Lasers '84, 681 1985.

QIFEL045/85: THE UCSB ELECTROSTATIC ACCELERATOR FEL: FIRST OPERATION
(Elias, Hu, Ramian)
Nuclear Instruments and Methods in Physics Research, A237, 203, 1985.

QIFEL046/85: FEL IN SMALL SIGNAL REGIMEN WITH A GAUSSIAN MODE
(Bernadini, Boscolo, Gallardo)
Nuclear Instruments and Methods in Physics Research, 1985.

QIFEL047/85: RAMAN-NATH EQUATION AND CLASSICAL DIFFUSION ONE-DIMENSIONAL RANDOM CHAIN
(Dattoli, Gallardo)
Phys. Rev. B, B31, 1608, 1985.

QIFEL048/85: INCOHERENT EMISSION OF AN ELECTRON BEAM IN A FEL RACTENGULAR WAVEGUIDE
(Elias, Gallardo, Gregoire)
J. Appl. Phys. 58 (4), August 1985.

QIFEL049/85: COMMENT ON PHOTON ANTIBUNCHING IN A FEL
(Dattoli, Gallardo, Richetta)
Phy. Rev. A., 32, 5, 3134, 1985.

QIFEL051/85: RECIRCULATING ELECTROSTATIC ACCELERATORS
(Elias, Ramian)
Transactions on Nuclear Science, IEEE, 5,
1732 OCT. 1985.

QIFEL052/85: OBSERVATION OF POWER INSTABILITY AND MULTIMODE BEHAVIOR IN THE UCSB FREE ELECTRON LASER
(Amir, Elias, Gregoire, Hu, Kotthaus,
Ramian, Stern) Applied Phys. Lett. 47(12)
15 Dec. 1985.Optical instabilities, eds. R.W.
Boyd, M.G. Raymer, L.M. Narducci, 249-252.

QIFEL053/86: FREE ELECTRON LASERS AND MAGNETIC MATERIALS
(L. Elias, I. Kimel, G. Ramian)
Journal of Magnetism and Magnetic Matl's
54-57, 1645 (1986)

QIFEL054/86: MAGNETIC TAPE UNDULATORS
(I. Kimel, W. Yen)
Journal of Magnetism and Magnetic Matl's,
54-57, 1471 (1986)

QIFEL059/85: SPONTANEOUS EMISSION IN THE WAVEGUIDE FEL
(Amir, Boscolo, Elias)
Phys. Rev. A, 32, 5, 2864, 1985.

QIFEL061/86: MULTIMODE DYNAMICS IN A FEL W/ENERGY SHIFT (Elias, Gallardo)
Lake Tahoe, Nuclear Instruments and Methods
in Phy. Res. A250 (1986)

QIFEL062/85: MICRO-UNDULATORS FELF
(G. Ramian, L. Elias, I. Kimel)
Lake Tahoe, Nuclear Instruments and Methods
in Phy. Res. S250 (1986)

QIFEL063/86: THE UCSB TWO-STAGE EXPERIMENT
(L. Elias, I. Kimel, Ramian)
Lake Tahoe, Nuclear Instruments and Methods in Phy. Res. A250 (1986)

QIFEL064/86: OBSERVATION OF SINGLE MODE OPERATION IN AN FEL
(Amir, Elias, Hu, Ramian)
Phy. Rev. Lett. Vol. 57 #4 7-28-86.

QIFEL065/86: COMMENTS ON QUANTUM MECHANICAL TREATMENT ON FELS IN THE LABORATORY FRAME
(Dattoli, Gallardo, Richetta)
Not Published

QIFEL066/86: COMMENTS ON EXACT SOLUTIONS FOR A ONE-DIMENSIONAL PERIODIC SOLID
(Dattoli, Gallardo, Richetta)
Journal of Math. Phys., 28, (2) Feb. 1987

QIFEL069/86: LASER LINE BROADENING DUE TO CLASSICAL AND QUANTUM NOISE AND THE FREE ELECTRON LASER LINEWIDTH
(A. Amir, L. Elias, A. Gover)
Phys. Rev. Letters 35, 1, 164-173 (1987)

QIFEL070/86: FREE ELECTRON LASER GAIN DEGRADATION AND ELECTRON BEAM QUALITY
(W. B. Colson, J. Gallardo, M. Bosco)
Phys. Rev. A A34, 4875 (1986)

QIFEL071/86: INSTABILITY IN A MULTIMODE FREE ELECTRON LASER: EFFECTS OF ENERGY DRIFT
(L. Elias, J. Gallardo, G. Dattoli, Alberto Renieri)
Phys. Rev. A 34, 3088 (1986)

QIFEL072/86: THREE-DIMENSIONAL THEORY OF THE FREE ELECTRON LASER I. GAIN AND EVOLUTION OF OPTICAL MODES
(A. Amir, Y. Greensweig)
Phys. Rev. A 34, 4809 (1986)

QIFEL073/86: THREE-DIMENSIONAL THEORY OF THE FREE ELECTRON LASER II. OPTICAL-MODE TRAPPING
(A. Amir, Y. Greensweig)
Phys. Rev. A, 34, 6, Dec. 86.

QIFEL083/87: NARROW-BAND RADIATION FROM LONG-PULSE FREE-ELECTRON LASERS (I. Kimel and L. Elias)
Physical Review A35, 3818, 1987.

F. FIGURES

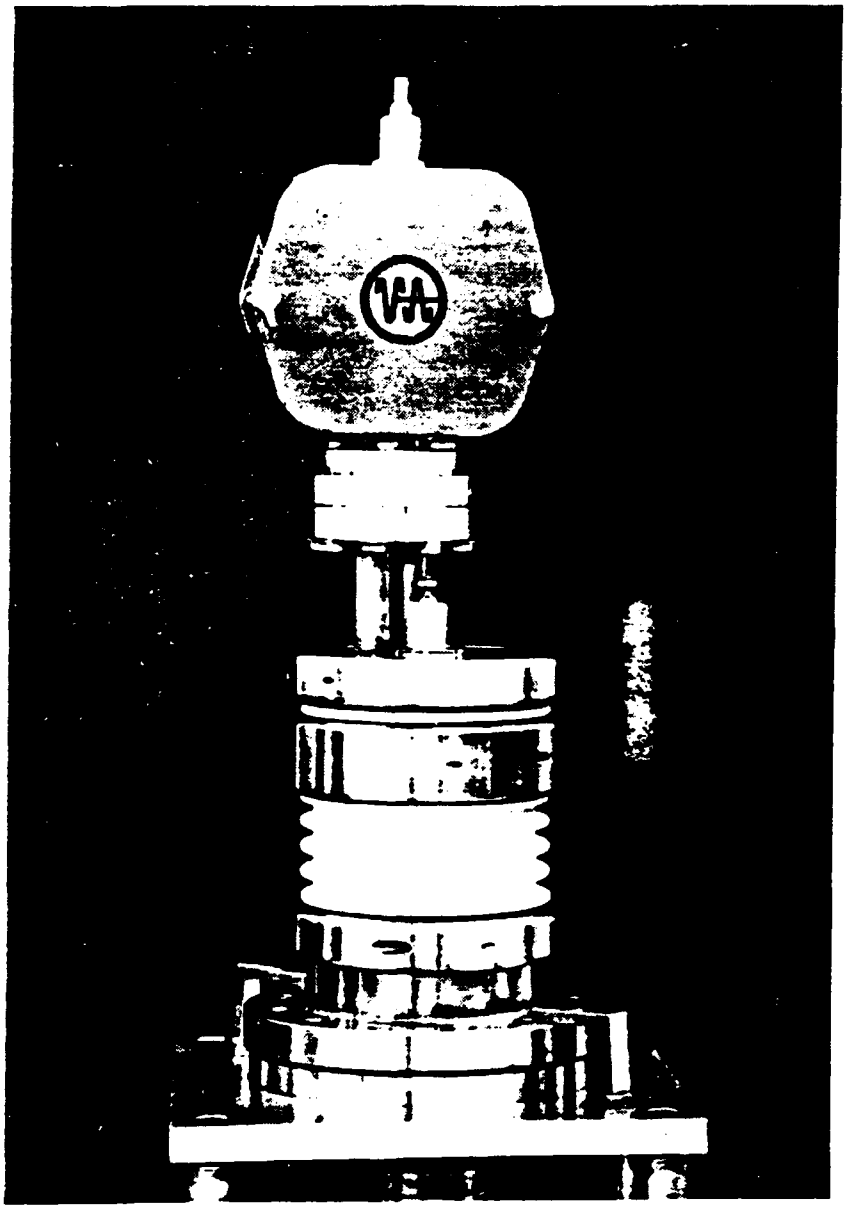

Figure 1. Photograph of the UCSB 2-Ampere electron gun.

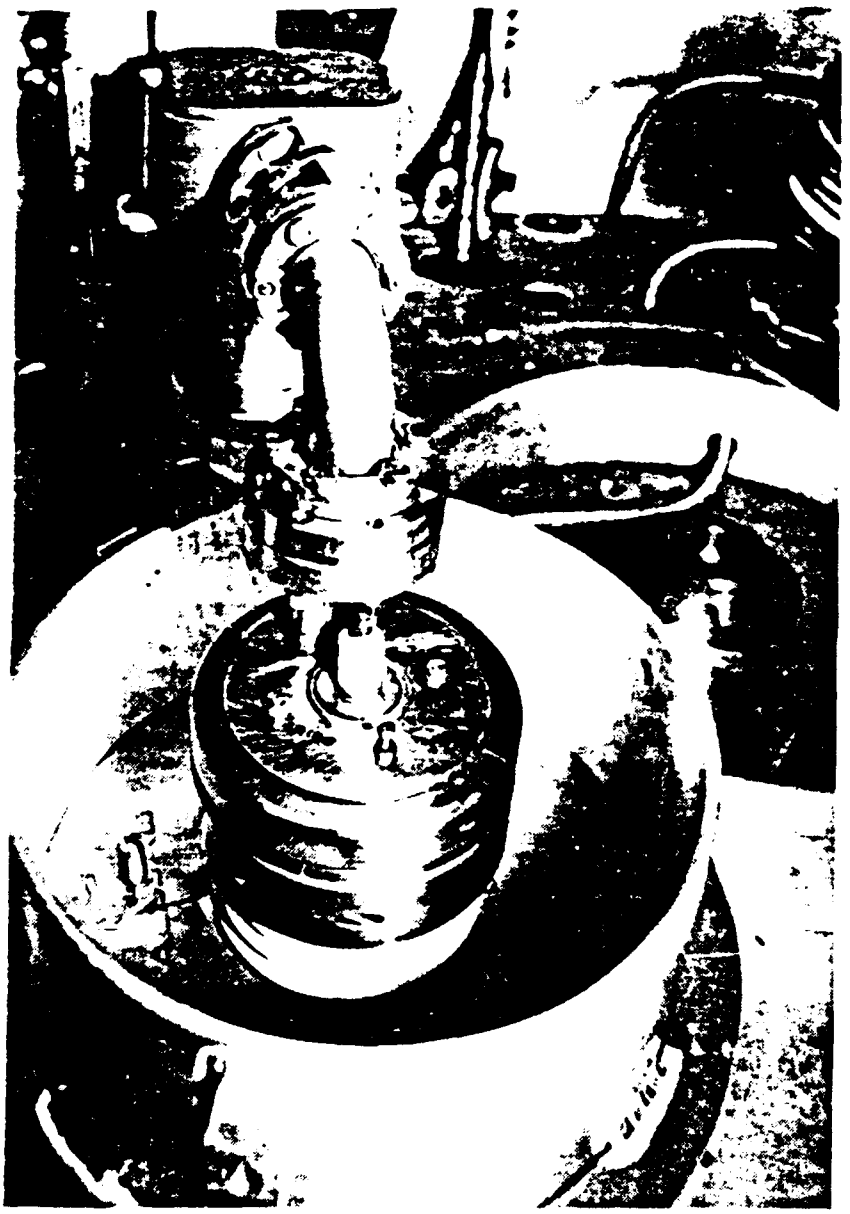

Figure 2. Photograph of the UCSB 2-Ampere electron gun installed inside the accelerator tank.

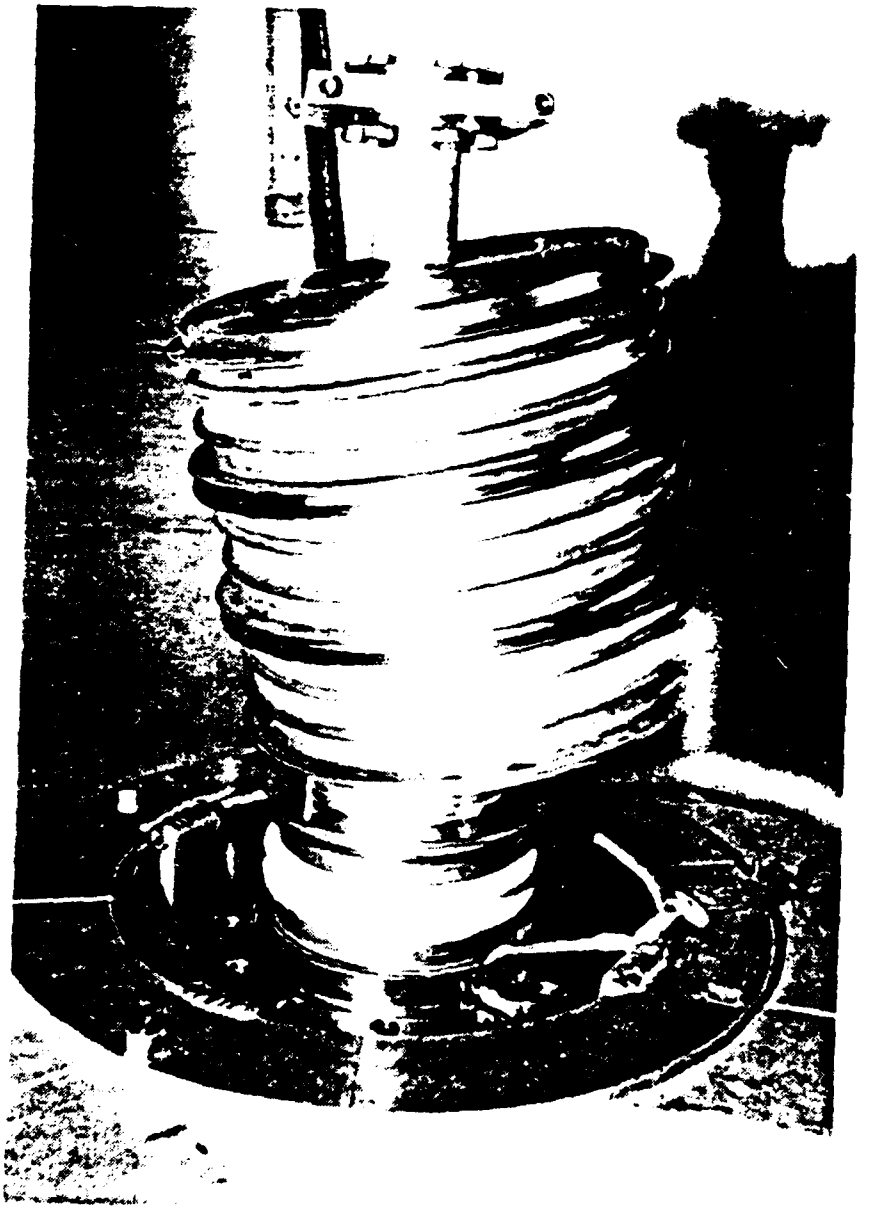

Figure 3. Photograph of the 2-Ampere electron collector inside the accelerator tank.

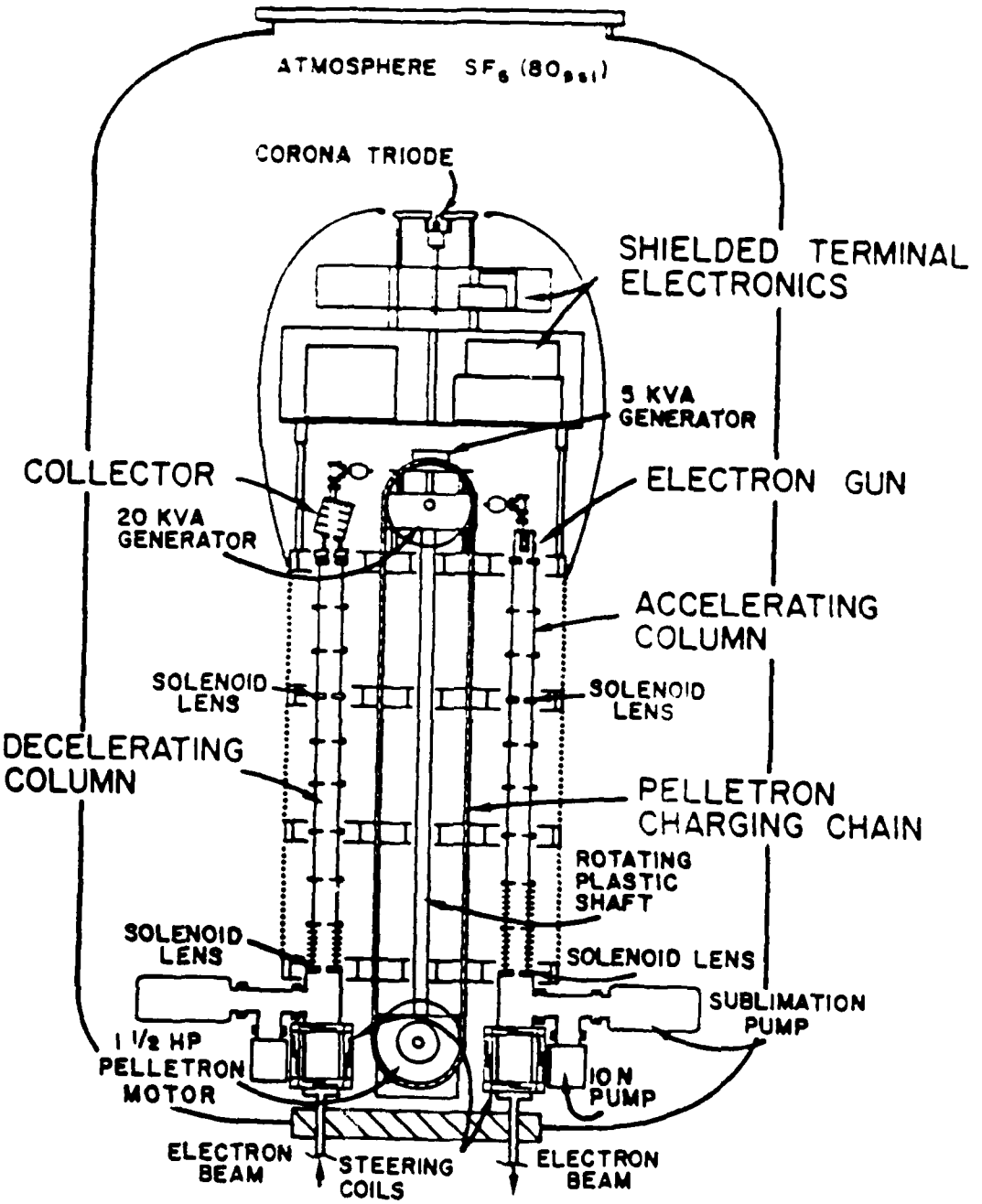

Figure 4. Major components of the UCSB electrostatic accelerator.

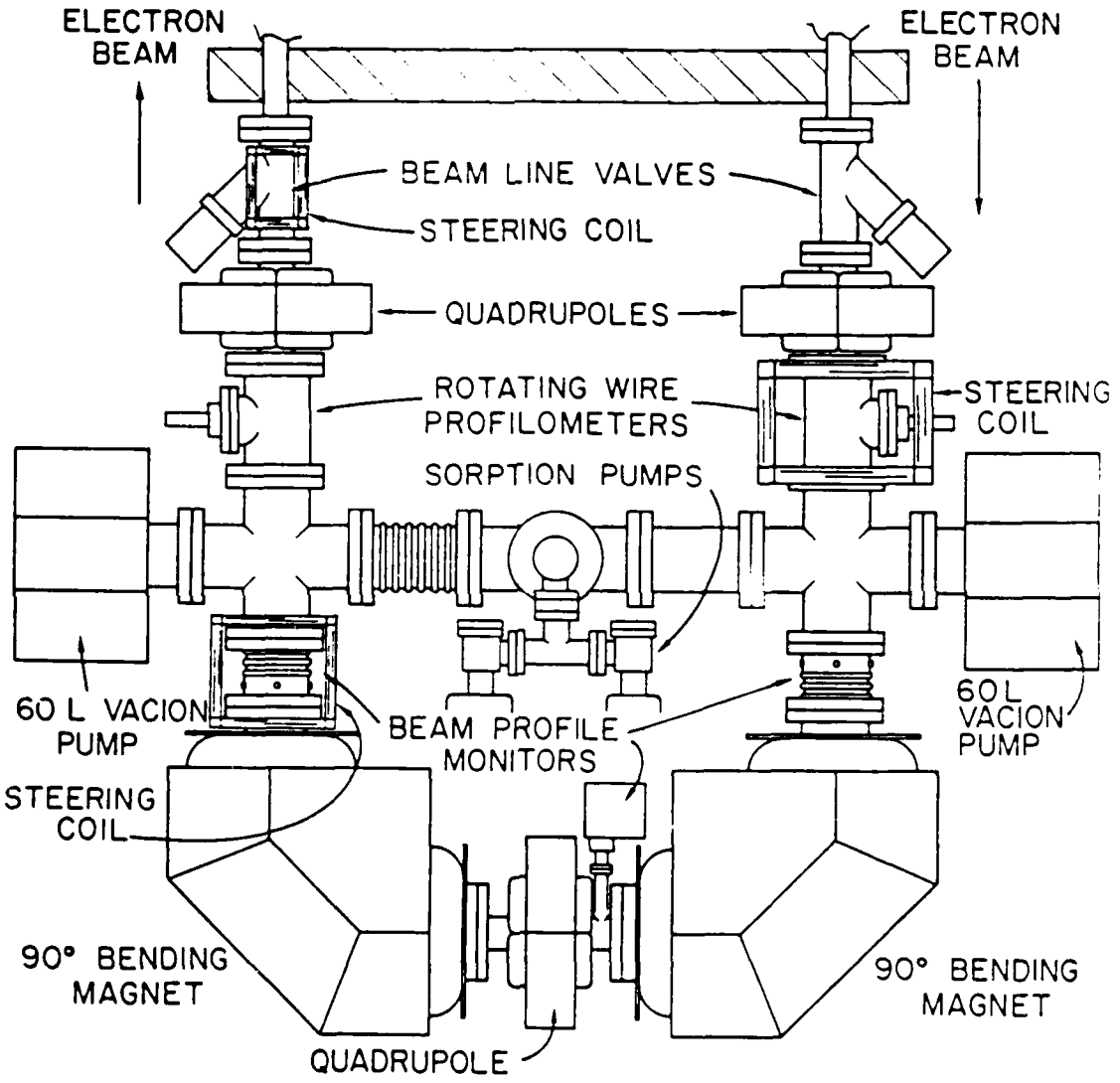

Figure 5. Electron beam recovery apparatus.

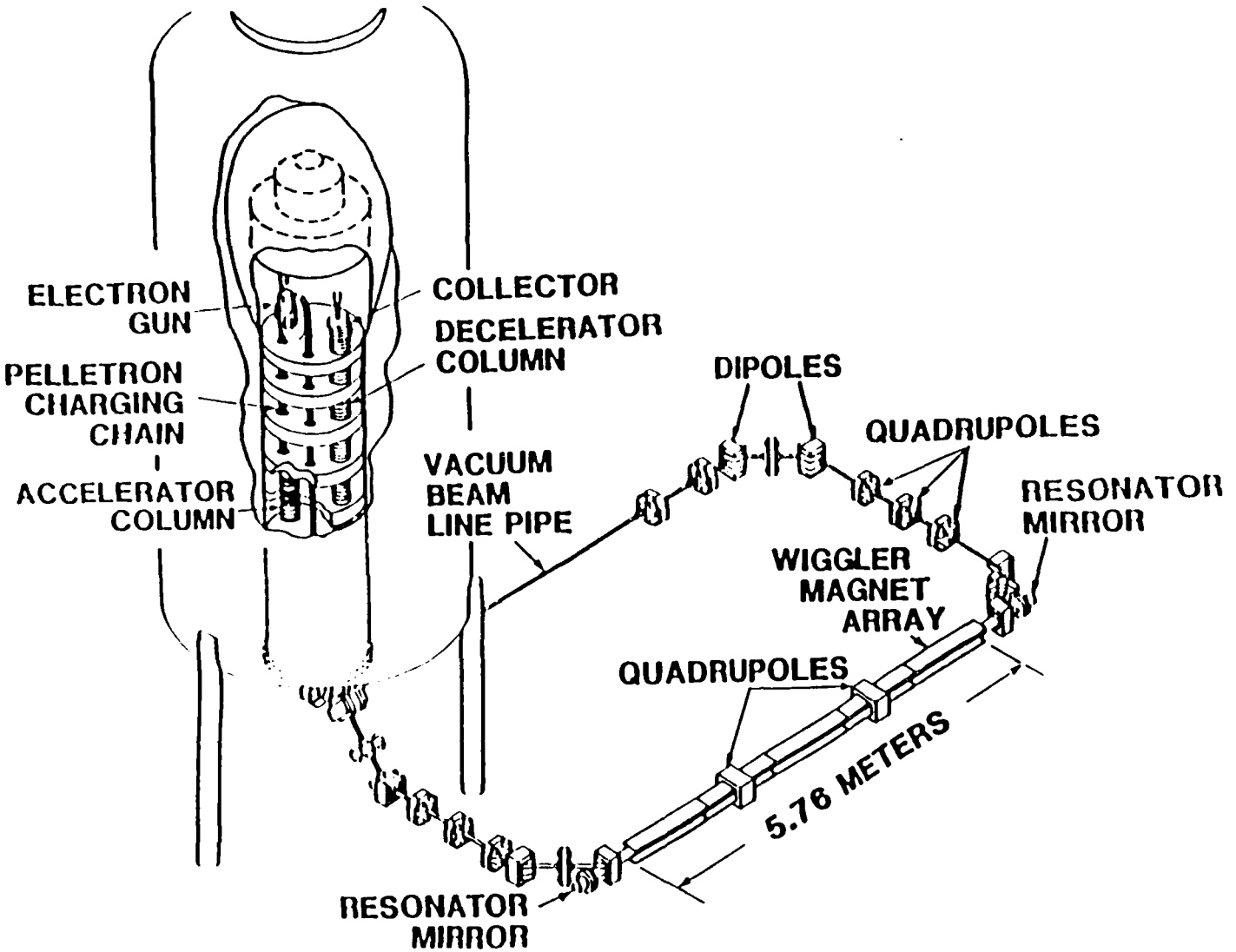

Figure 6. Layout of the accelerator and electron beam transport system.

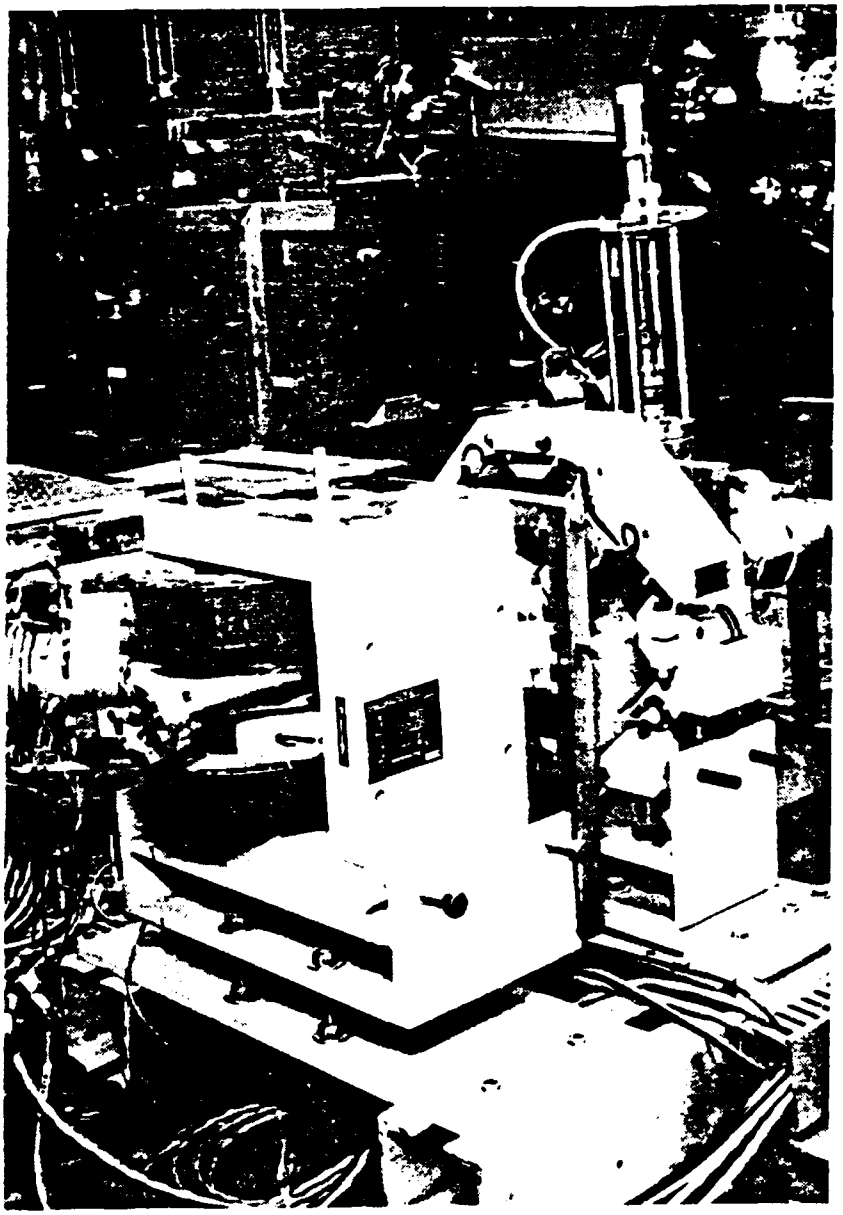

Figure 7. Photograph of a bending magnet and a quadrupole.

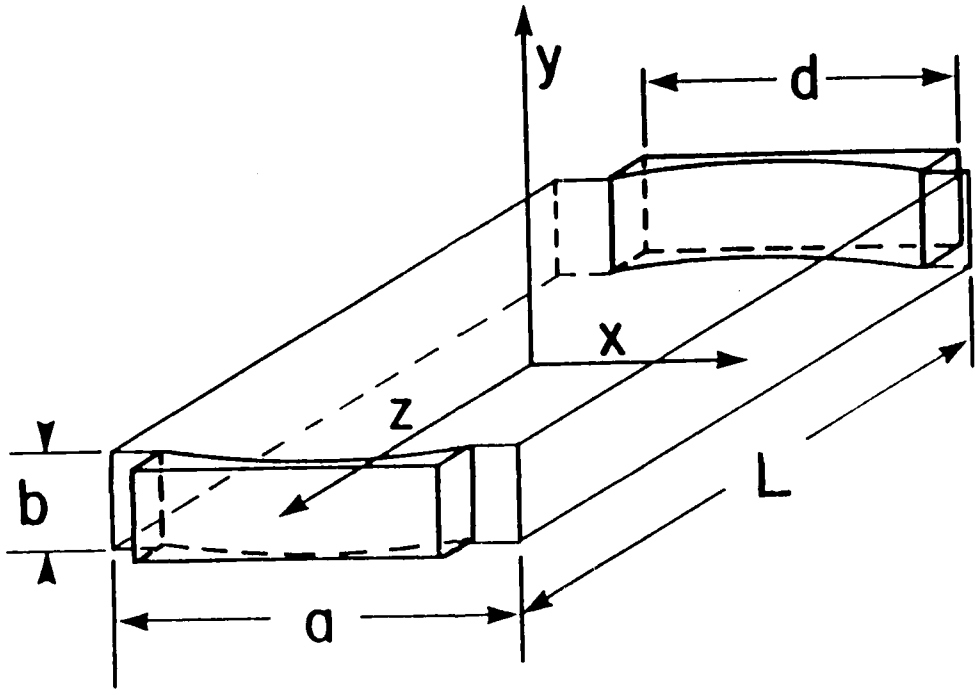

Figure 8. Geometry of UCSB FEL resonator.

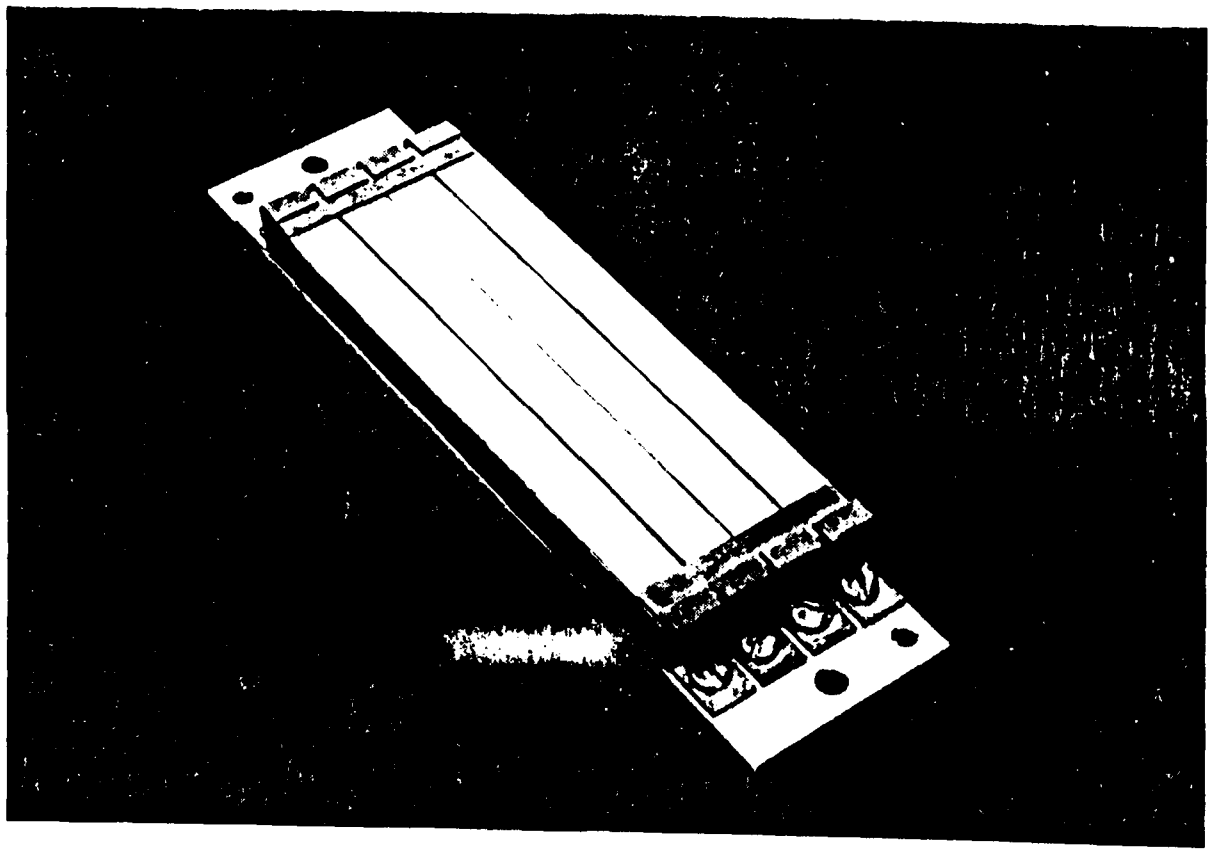

Figure 9. Undulator carrier plate with four magnets.

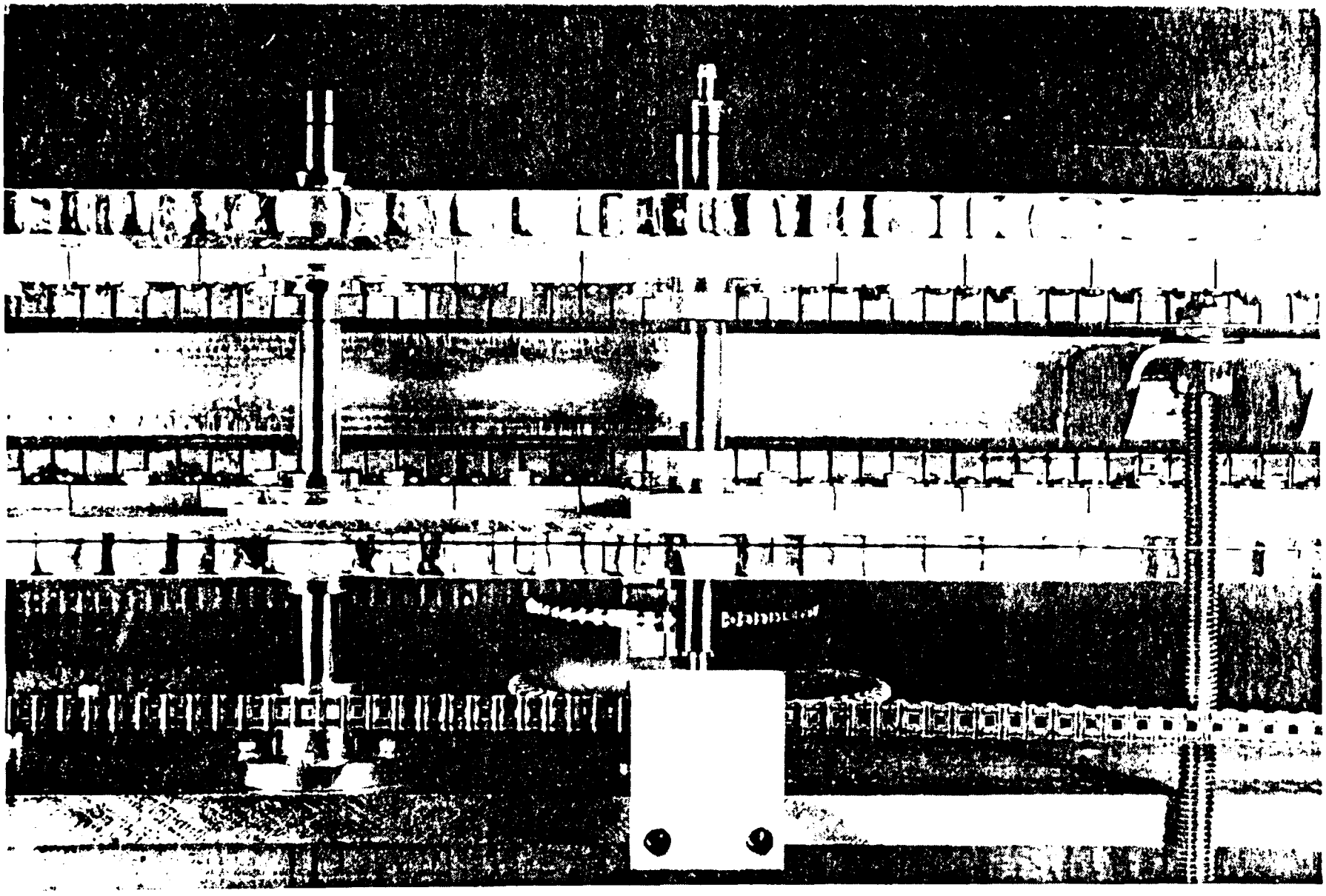

Figure 10. Side-view photograph of the UCSB linear undulator.

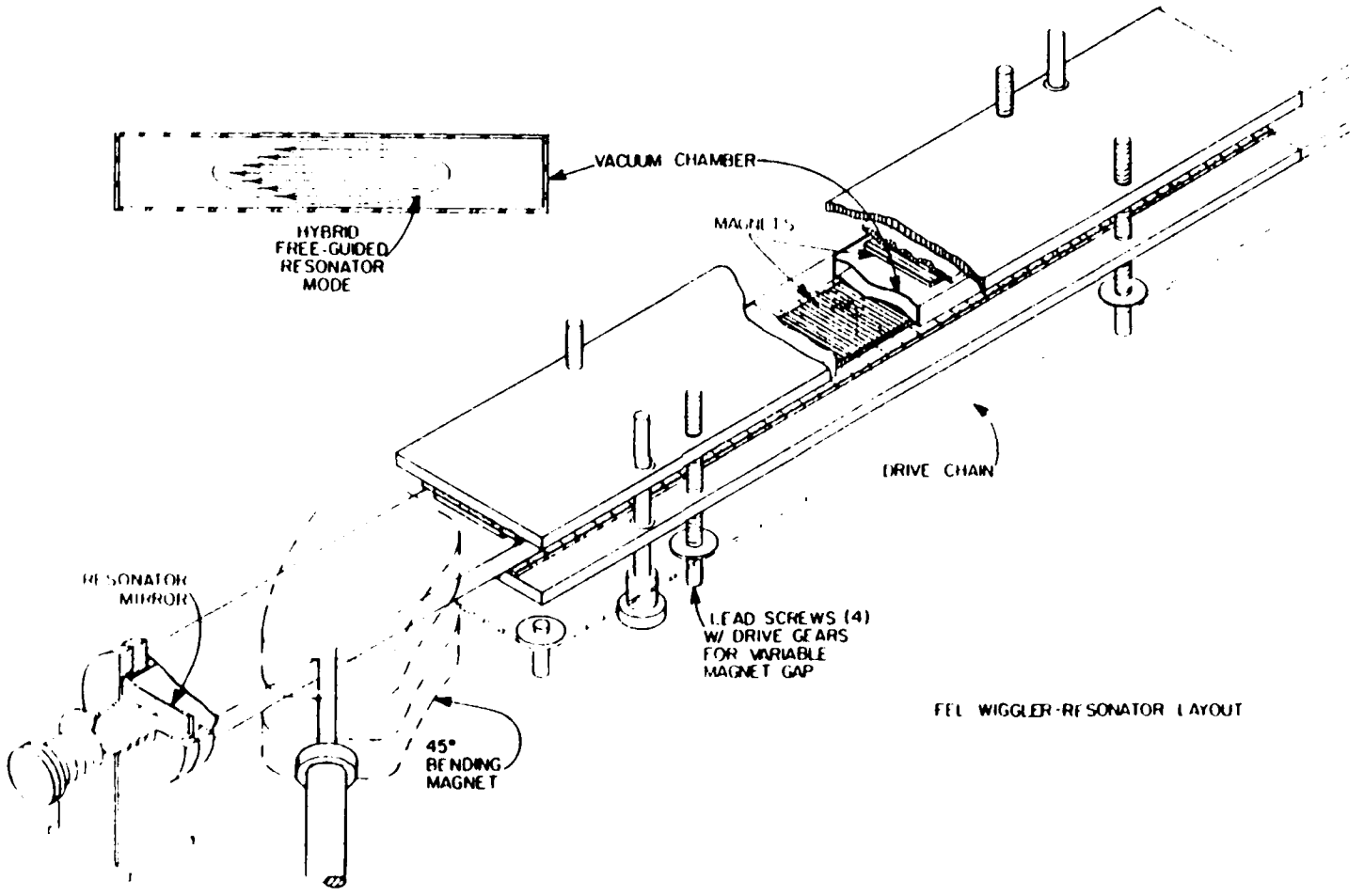

Figure 11. Major components of the FEL undulator.

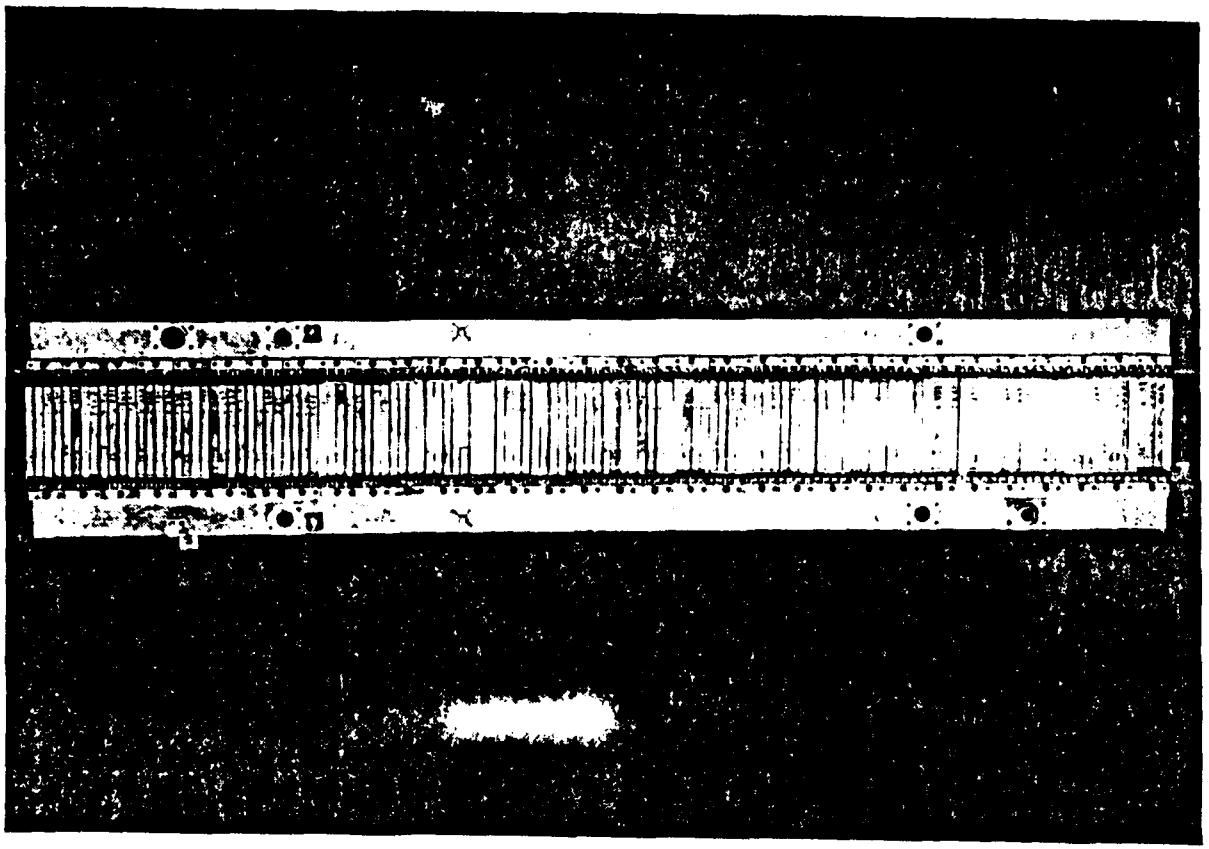

Figure 12. Photograph of a section of the FEL linear undulator with the top panel off.

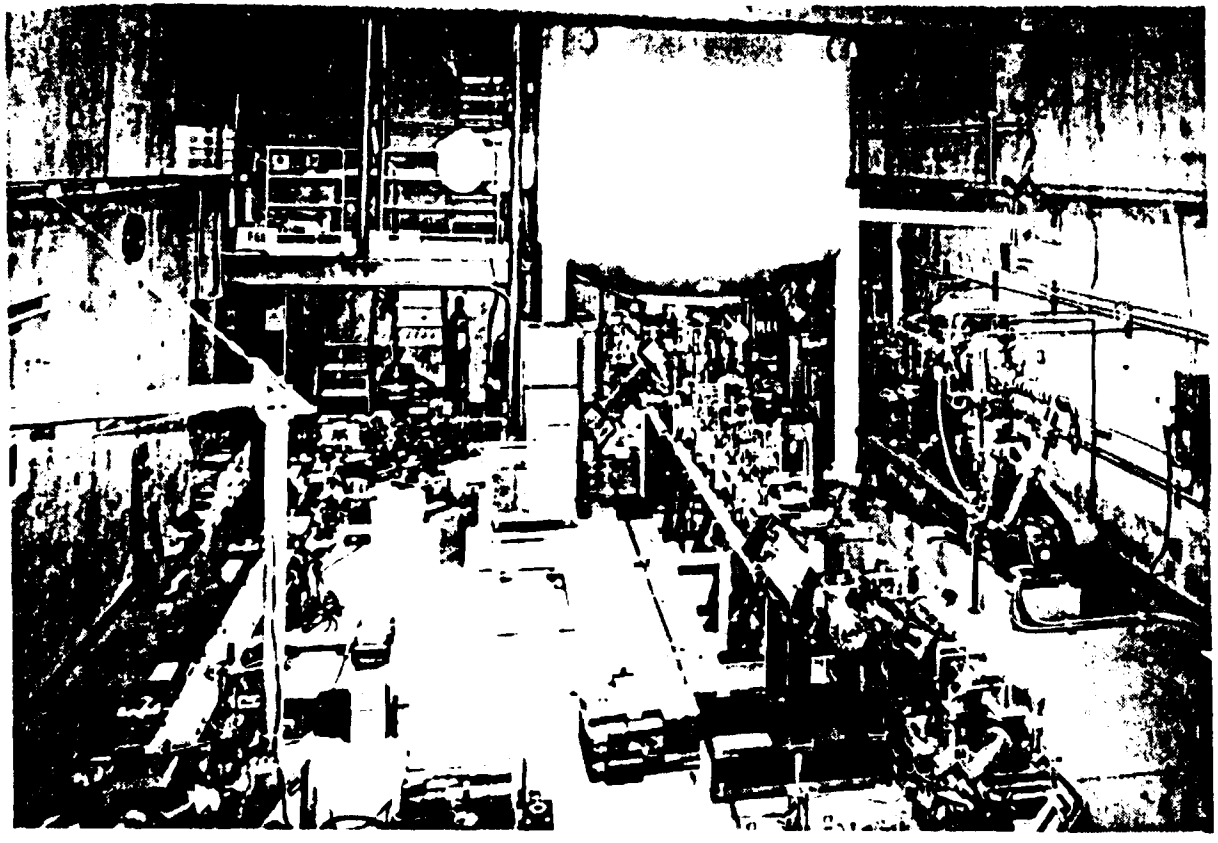

Figure 13. View of the FEL laboratory. The linear undulator is near (and parallel to) the left wall, the accelerator tank is in the background and the two-stage FEL to the right, next to the beam line bringing the electrons down from the accelerator.

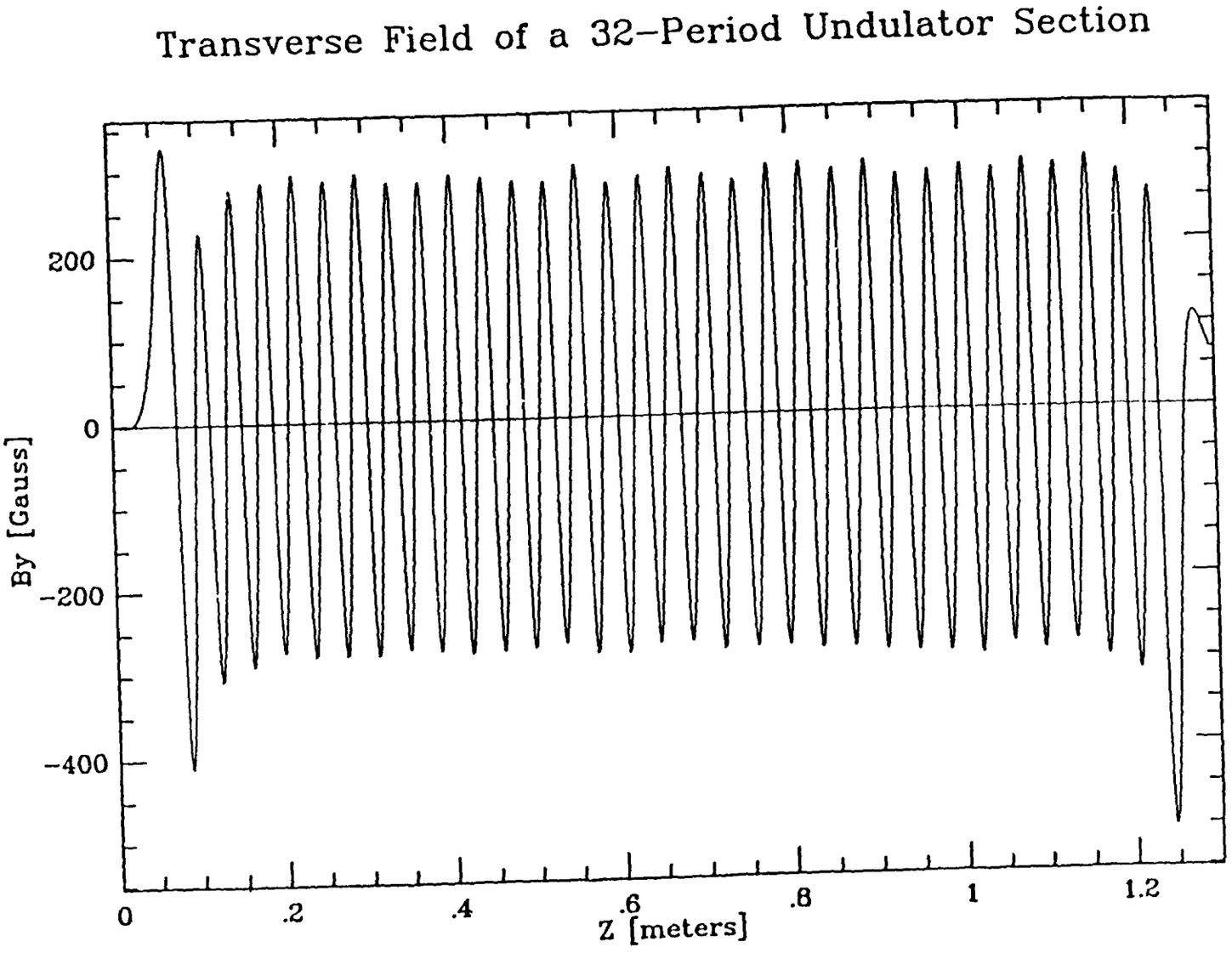

Figure 14. Transverse magnetic field on axis of a 32 period linear undulator section.

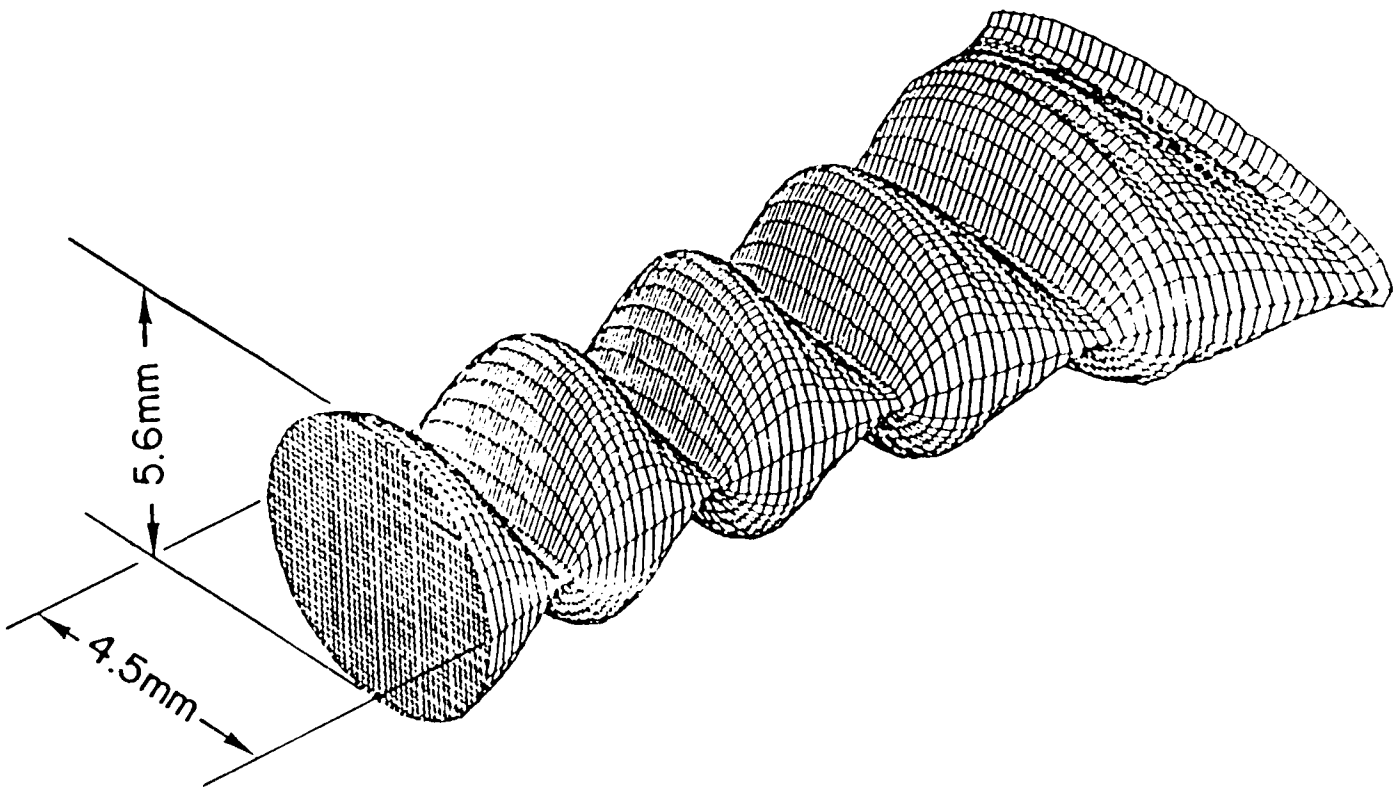

Figure 15. Electron beam envelope inside the UCSB linear undulator.

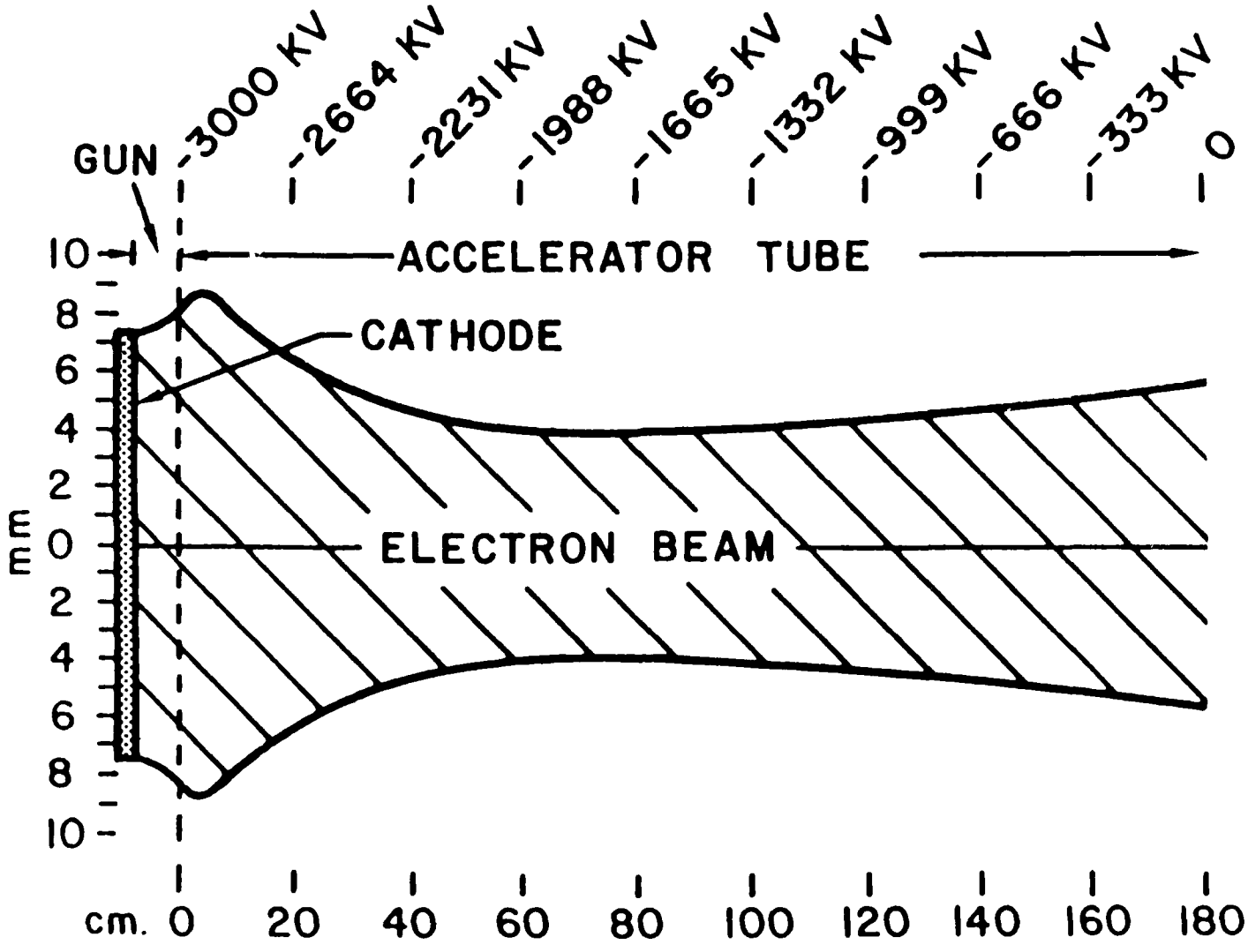

Figure 16. Electron beam optics inside an 3 MV NEC accelerator tube.

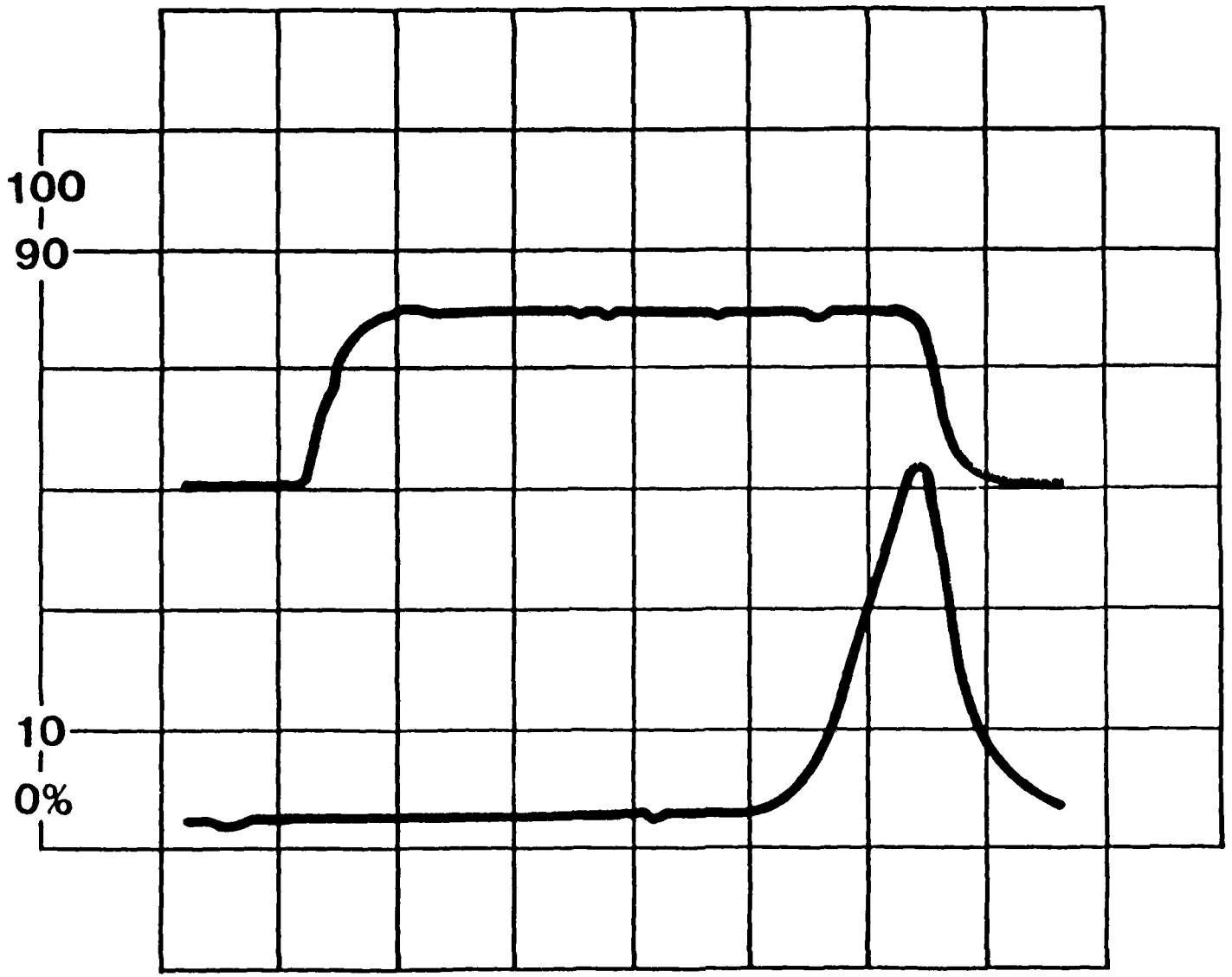

Figure 17. FEL power vs. time (lower trace) of a short electron beam pulse (upper trace). Horizontal scale is 1 μs/div.

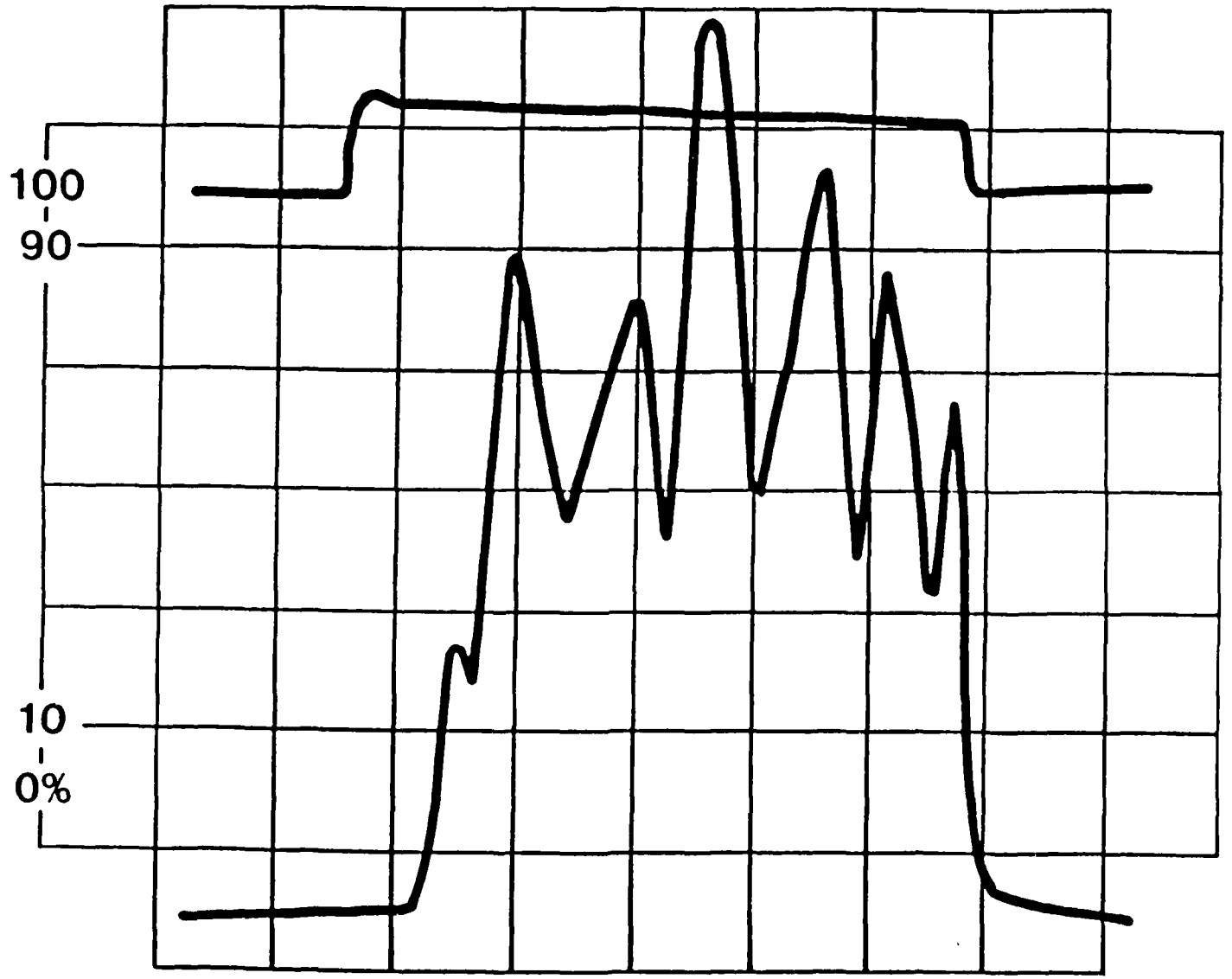

Figure 18. FEL power vs. time (lower trace) for a long electron beam pulse (upper trace). Horizontal scale is 0.25 μs div.

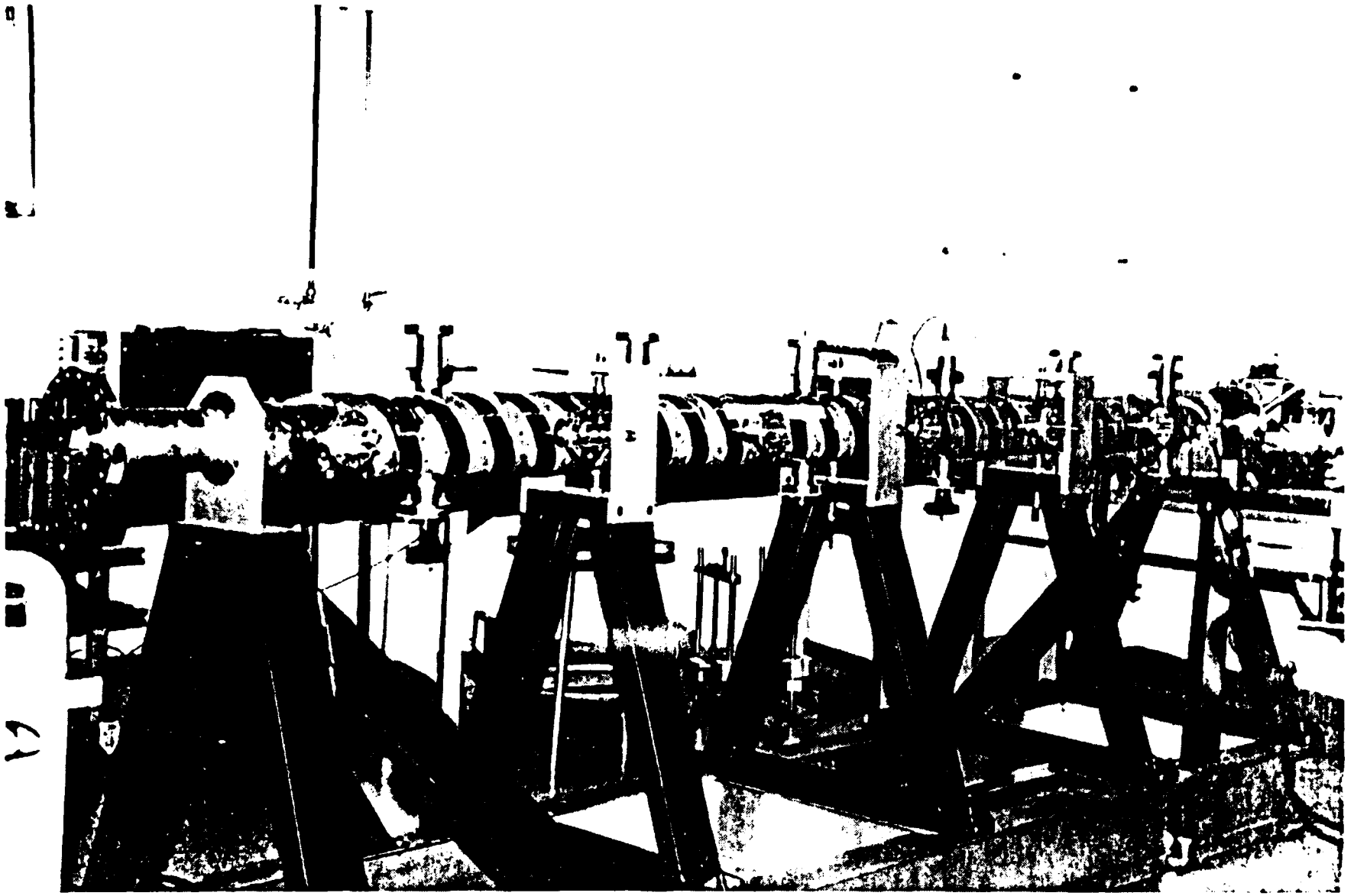

Figure 19. Photograph of the UCSB helical undulator.

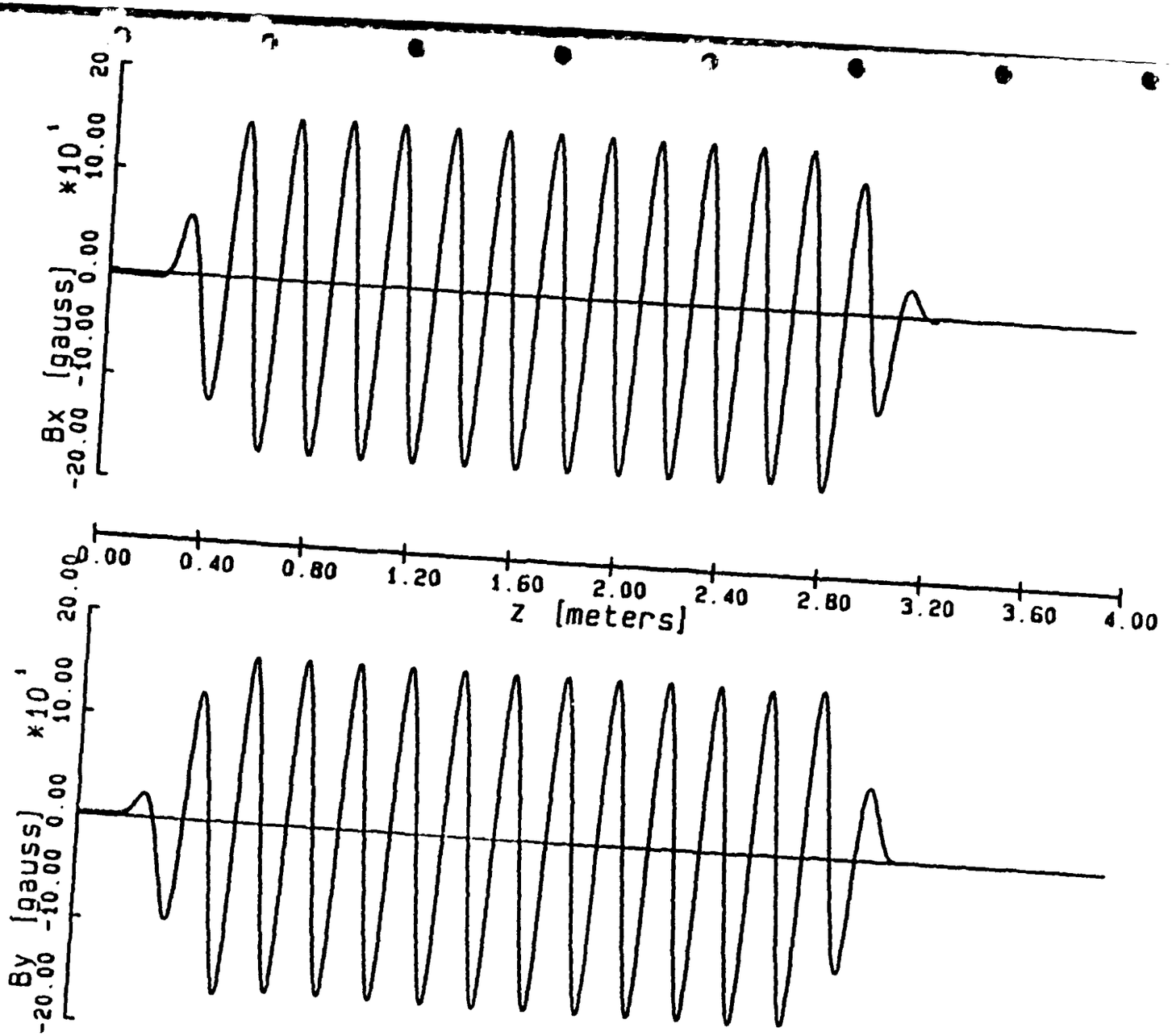

Figure 20. Transverse field on axis of the helical undulator.

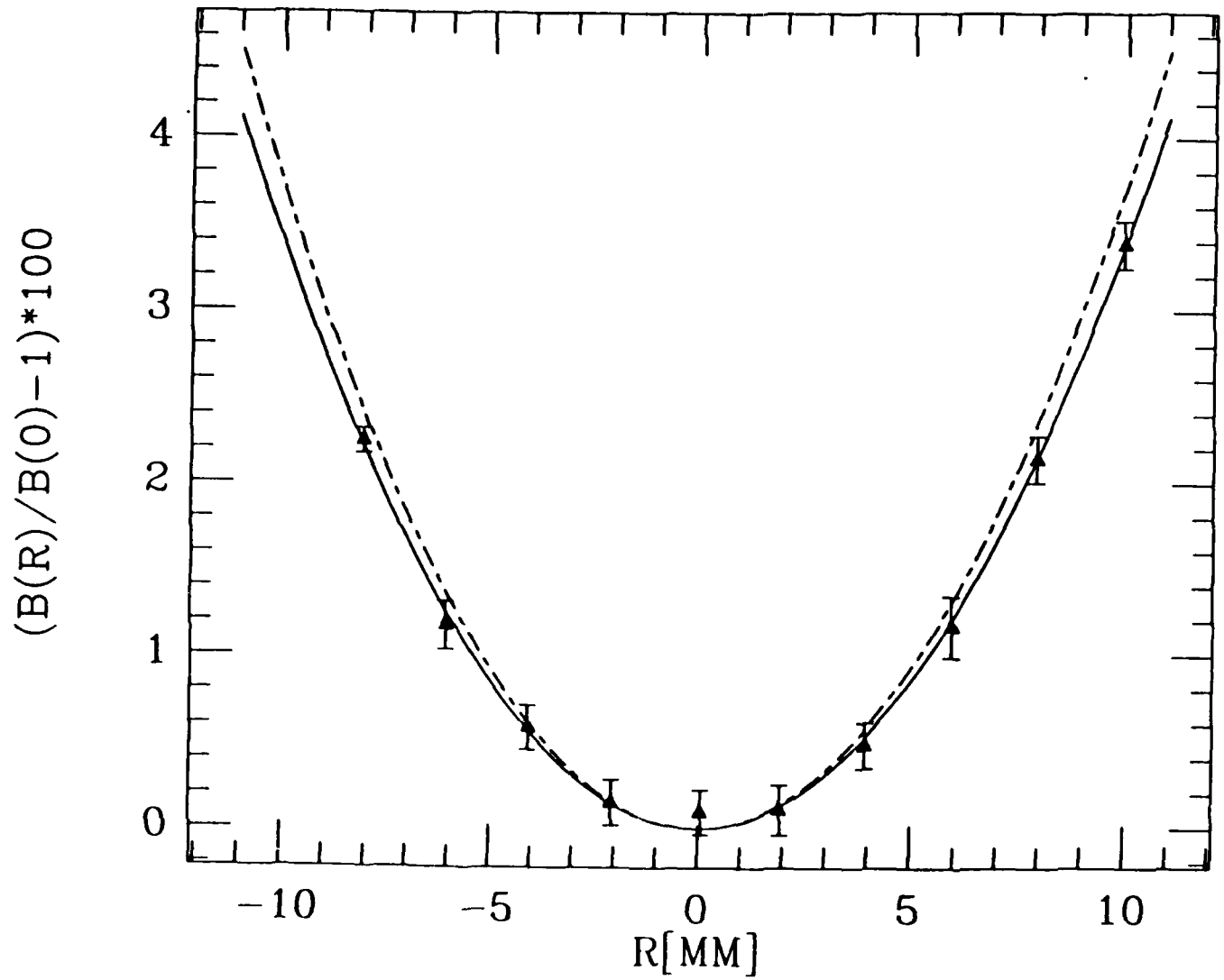

Figure 21. Transverse field as a function of distance from the helical undulator axis.

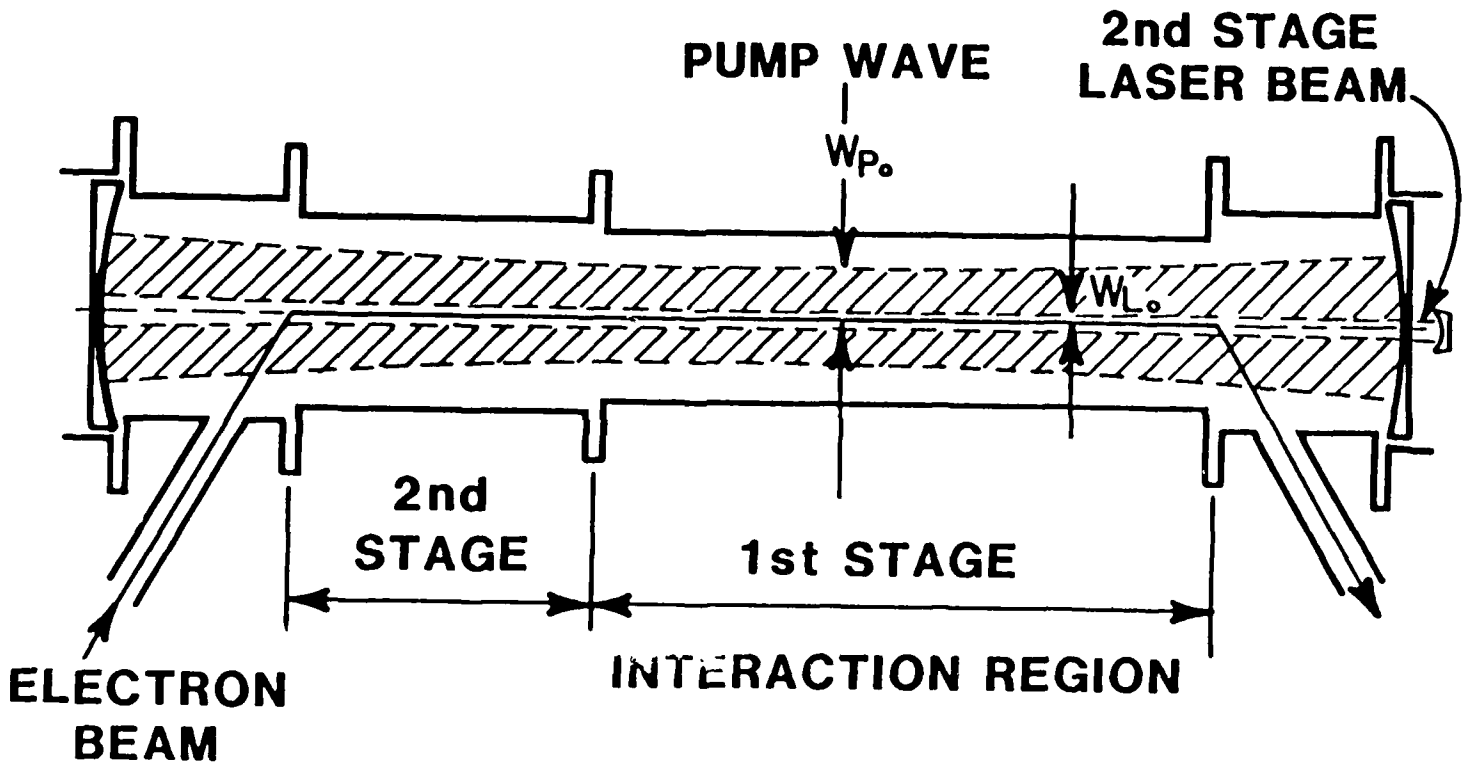

Figure 22. Resonator optics for the the two-stage FEL.

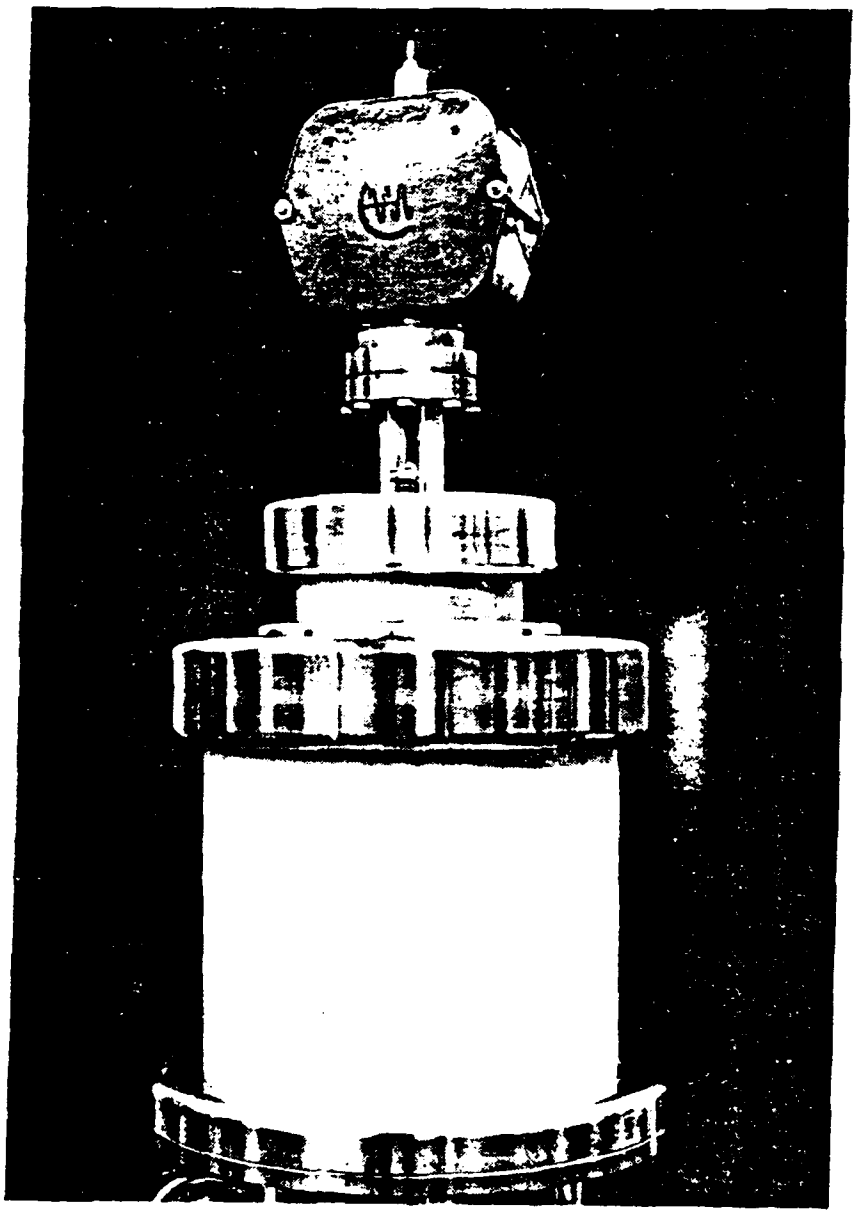

Figure 23. 20-Ampere, 200 kV, electron gun photograph.

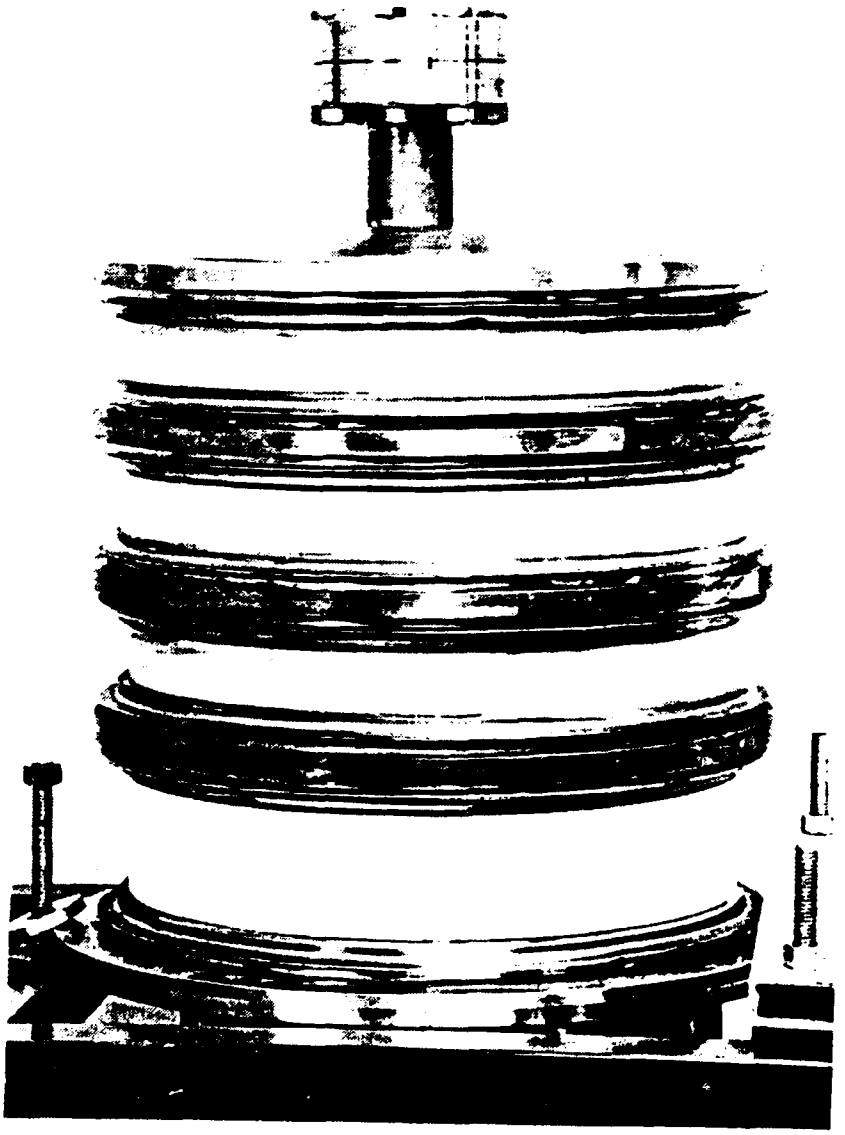

Figure 24. 20-Ampere, 200 kV, multistage electron collector photograph.

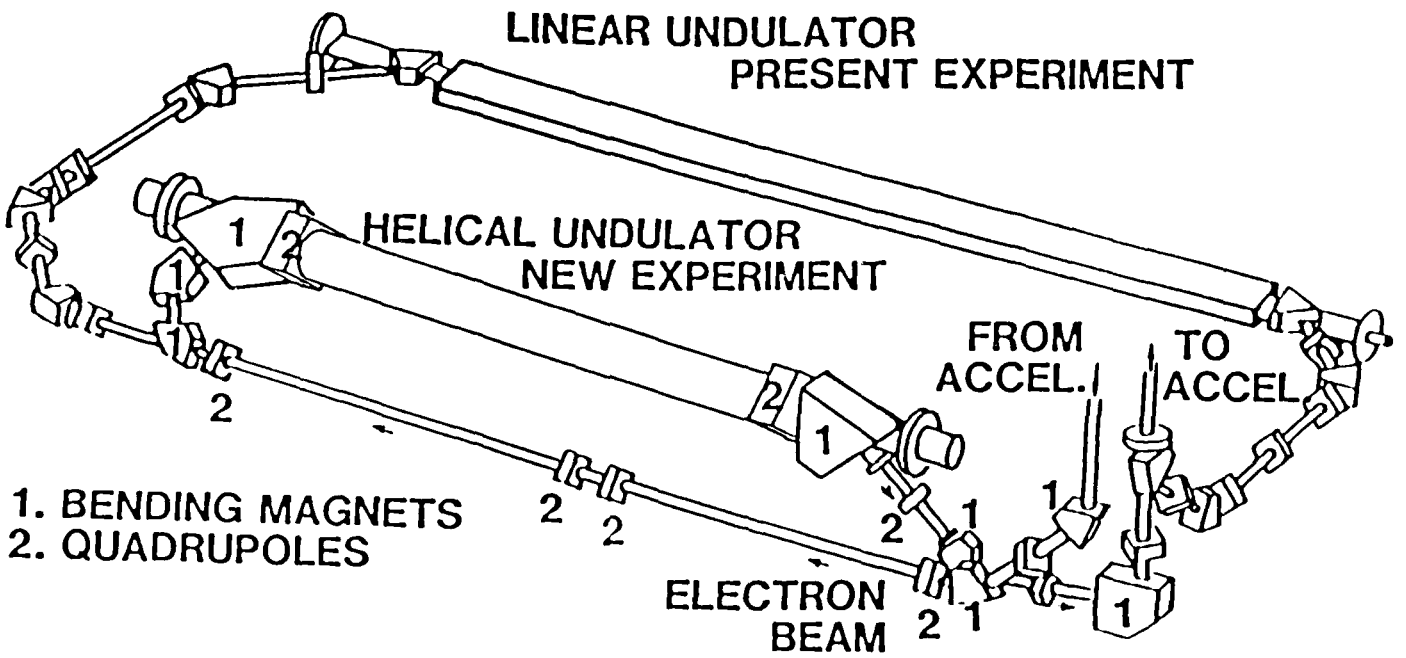

Figure 25. Schematic layout of the new two-stage beam line together with the single stage beam line.

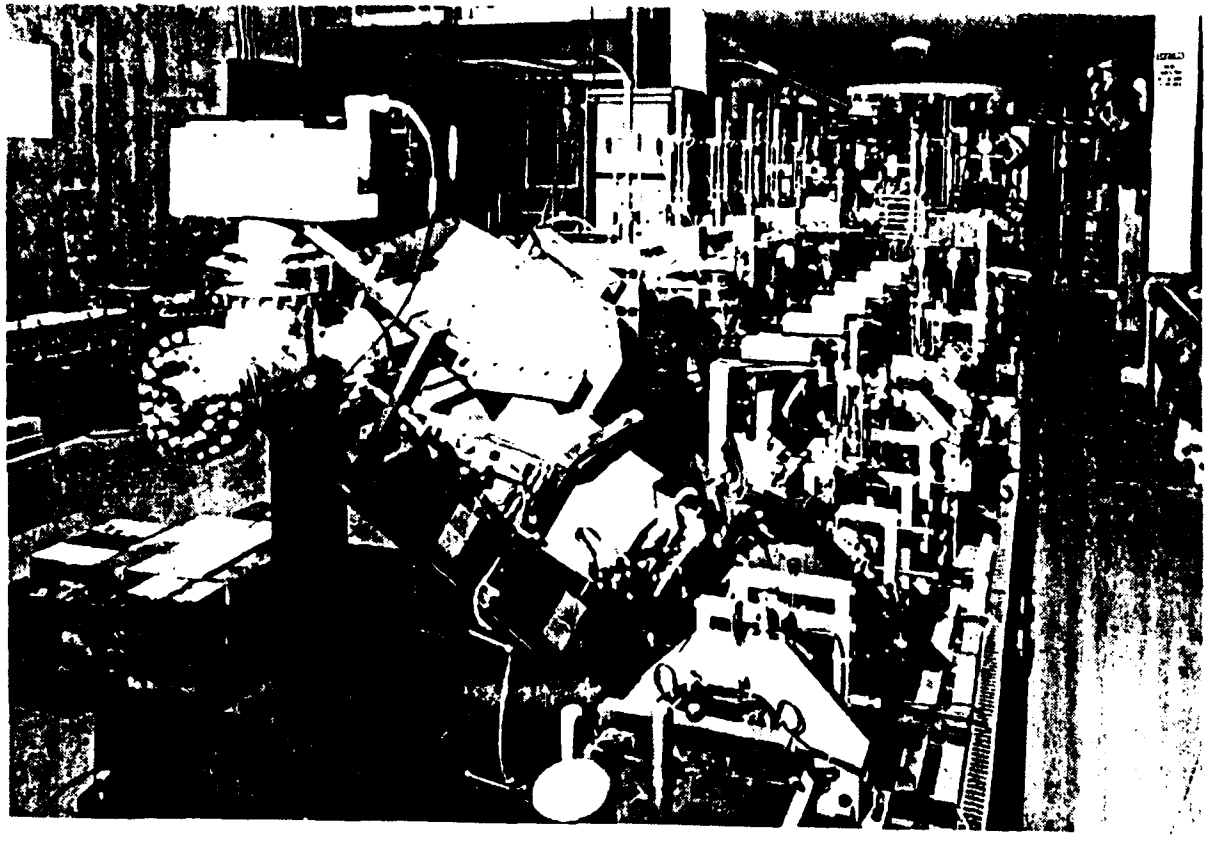

Figure 26. Hardware for the first stage of the two-stage FEL.

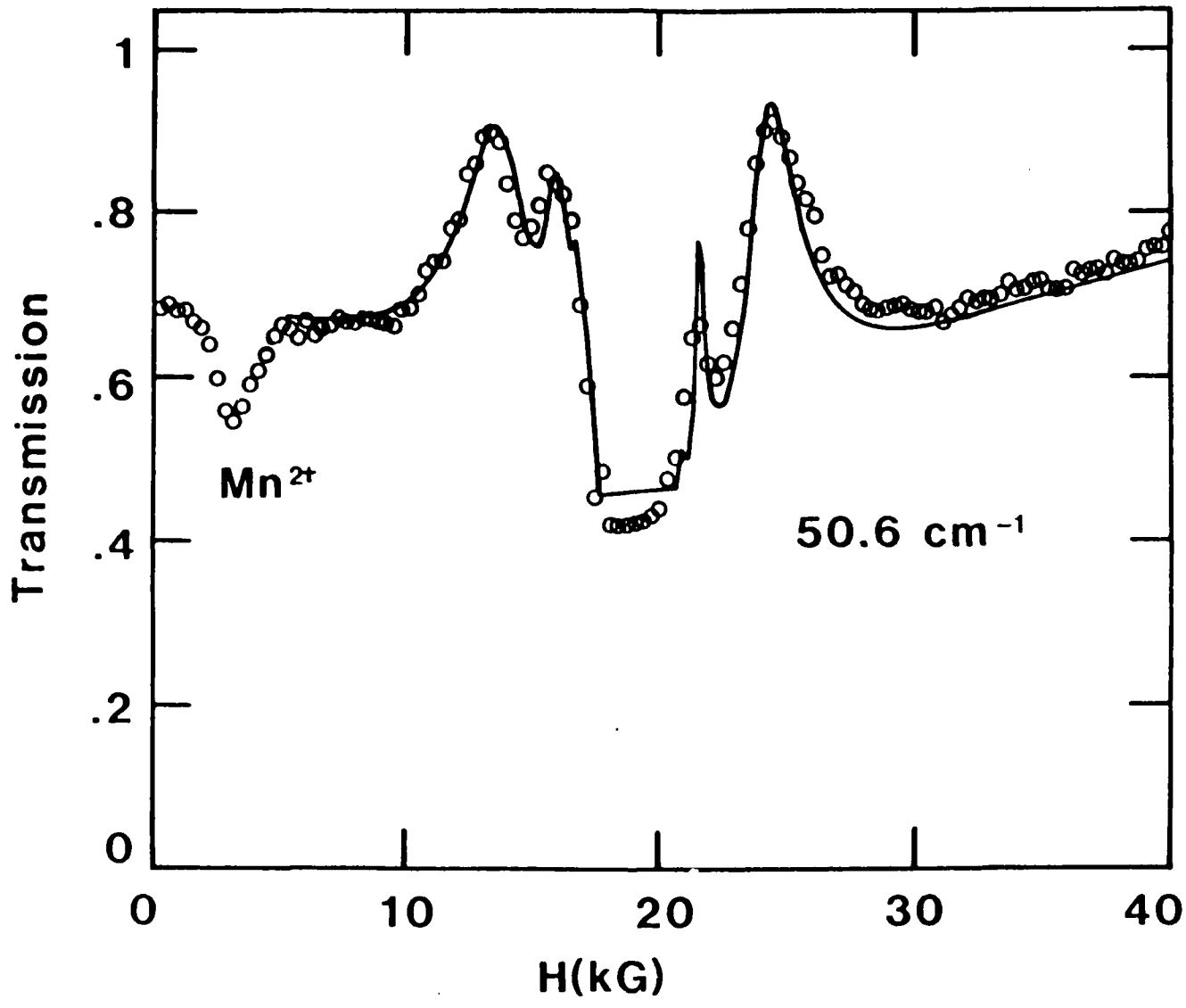

Figure 27. Transmission spectra of FeF_2.

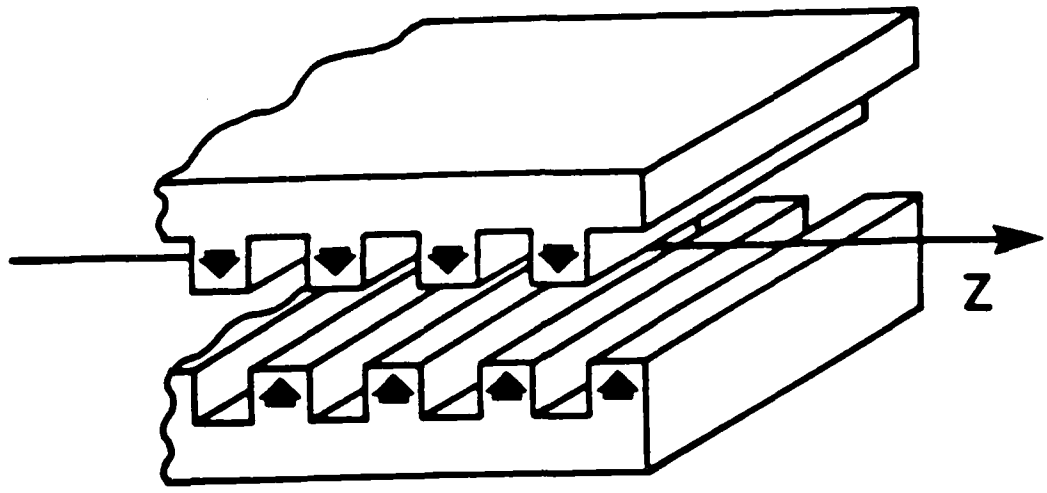

Figure 28. Microundulator design with magnetization perpendicular to undulator axis.

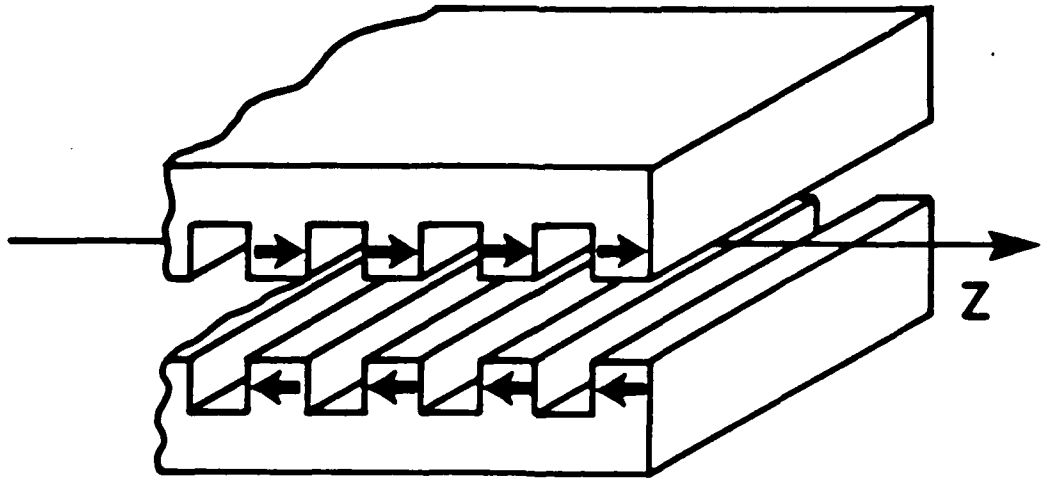

Figure 29. Microundulator design with magnetization parallel to undulator axis.

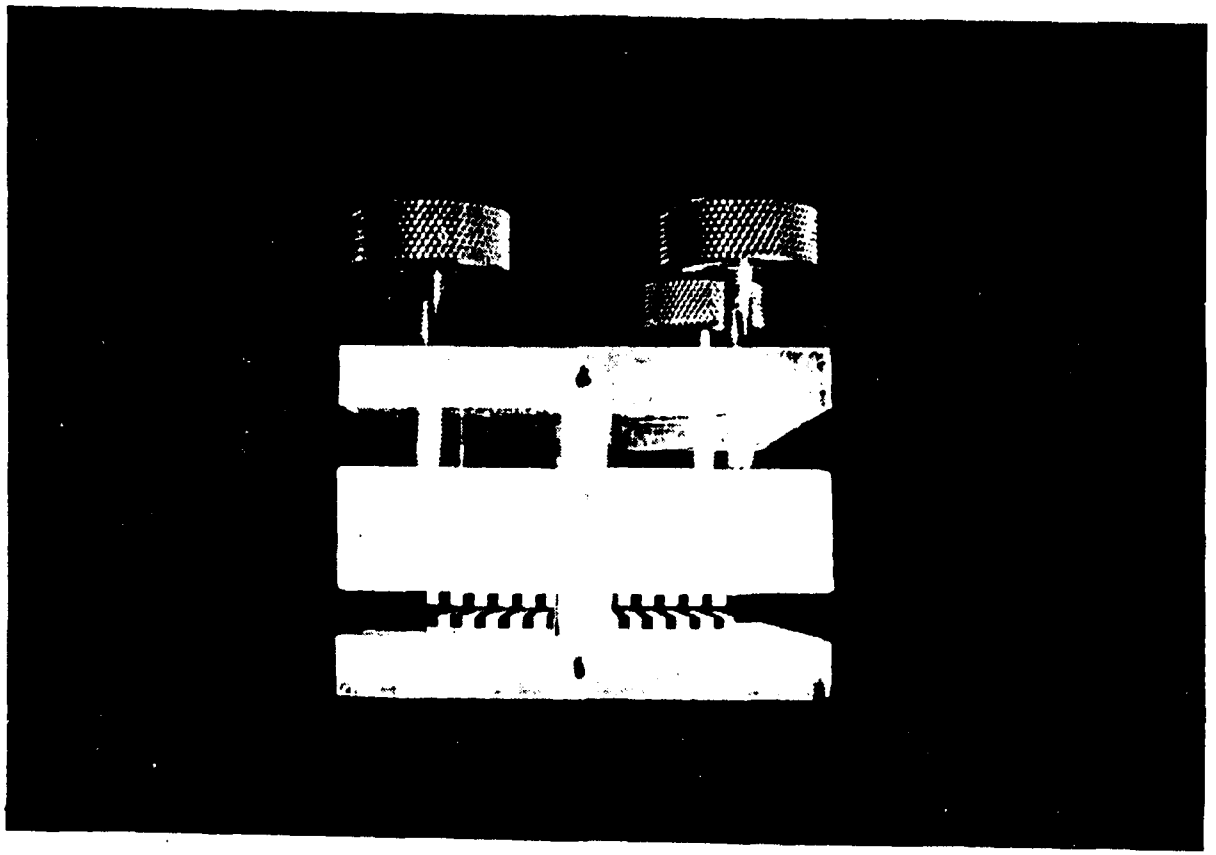

Figure 30. Photograph of microundulator section.

A COMPACT SUBMILLIMETER FEL IS UNDER DEVELOPMENT AT UCSB

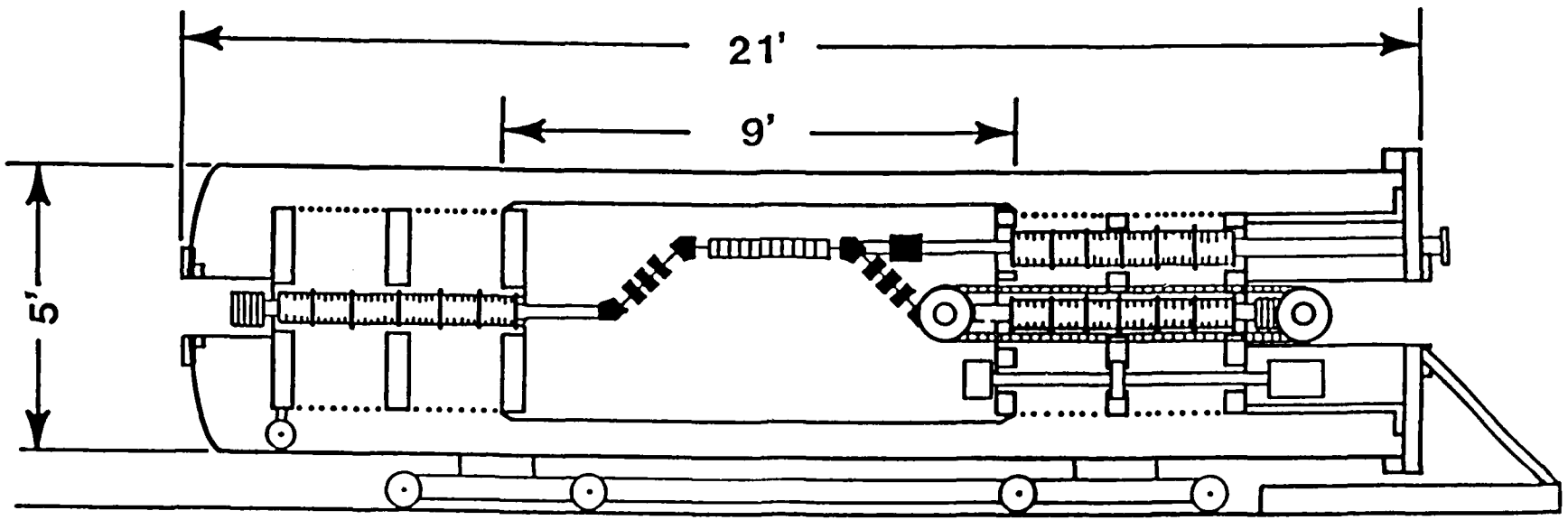

Figure 31. A compact 2-MeV FIR FEL using microundulators.

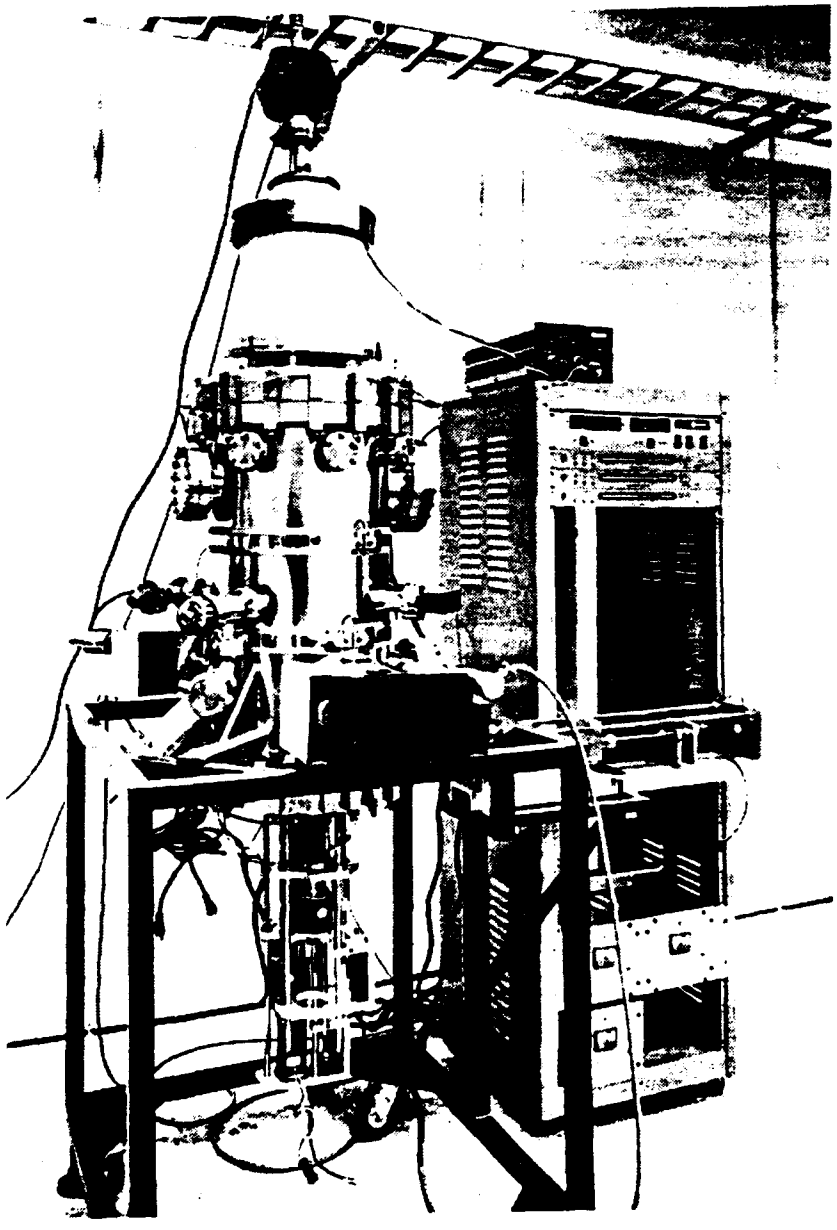

Figure 32. Photograph of the UCSB electron beam analyzer hardware.

END

DATE

3-88

DTIC